NEMESIS
Negative Effects in Medical Sciences Oral and Maxillofacial Surgery
UCL PRESSES UNIVERSITAIRES DE LOUVAIN

Diagnostic value of cone beam computed tomography in complex and compound odontomas: a systematic review and open classification matrix

Authors:
Dubron K MD,MM,DDS[1,2],
Gurniak A DDS[3],
Gurniak E DDS[3],
Politis C MD,DDS,MM,MHA,PhD,Prof[1,4]
Olszewski R DDS,MD,PhD,DrSc,Prof[2,5,*]

Affiliations:

[1] Department of Oral and Maxillofacial Surgery, University Hospitals Leuven, Kapucijnenvoer 33, 3000 Leuven, Belgium
[2] Department of oral and maxillofacial surgery, Cliniques universitaires saint Luc, UCLouvain, Av. Hippocrate 10, 1200 Brussels, Belgium
[3] Diagdent, ul. Brazylijska 13, Warszawa, Poland
[4] OMFS IMPATH Research Group, Department of Imaging & Pathology, University Hospitals Leuven, Belgium
[5] Oral and maxillofacial surgery research lab (OMFS Lab), NMSK, Institut de recherche expérimentale et Clinique (IREC), SSS, UCLouvain, Brussels, Belgium

*Corresponding author: Prof R. Olszewski, Department of oral and maxillofacial surgery, Cliniques universitaires saint Luc, UCLouvain, Av. Hippocrate 10, 1200 Brussels, Belgium, phone+3227645718; fax: +3227645876; ORCID iD:orcid.org/0000-0002-2211-7731

Disclaimer: the views expressed in the submitted article are our own and not an official position of the institution or funder.

Abstract

Objective: Firstly, this review aims to analyse the recent literature about three-dimensional (3D) diagnostic imaging in complex and compound odontomas and compare it to two-dimensional (2D) imaging. Panoramic radiographs help to evaluate the vertical position of odontomas, and occlusal radiographs are used to evaluate the proximity to adjacent teeth. However, cone beam computed tomography (CBCT) can offer volumetric images, and therefore, a more accurate three-dimensional analysis. Secondly, this research aims to construct an open classification matrix for complex and compound odontomas for dentomaxillofacial CBCT radiology protocols based on a systematic literature review.

Material and methods: Two systematic literature searches were conducted in PubMed (Medline), on 2 February 2022 concerning classification systems, and on 5 February 2022 concerning CBCT images.

Results: In total, these searches revealed 391 papers by reviewing the databases mentioned above. Six articles were selected for inclusion on classification of odontomas and 13 articles were found on CBCT imaging. Consequently, the construction of an open classification matrix for compound and complex odontomas for dentomaxillofacial CBCT radiology protocols was performed using these 19 articles.

Conclusions: CBCT offers a more precise position and accurate diagnosis of complex and compound odontomas compared to 2D imaging. Consequently, it enhances the detailed view of the site (multiple or unique), location (intraosseous, partially or completely extragnathic), size, extension (bony expansion, thinning or perforation cortical bone), density and type (denticulo type, particle type, denticulo-particle type, denticulo-amorphous type, amorphous tissue), relationship (with the crown or root of the definitive tooth), adjacent teeth resorption (deciduous or definitive), adjacent teeth (retention or impaction), and distance with adjacent structures (inferior alveolar nerve, sinus maxillaris), as well as adequate surgical planning. Moreover, this research presents an open classification matrix for the most complete description of compound and complex odontomas when analysing CBCT imaging.

Keywords: cone beam computed tomography, CBCT, complex odontoma, compound odontoma, odontogenic tumour

Introduction

Odontomas are the most common odontogenic tumours, according to the World Health Organization's (WHO) International Classification of Tumours. Odontomas are defined as malformations or hamartomas in which both epithelial and mesenchymal cells present complete differentiation with enamel formation and dentin [1]. However, all different tooth components can be found in an odontoma (enamel, dentine, cementum, dental follicle, and pulp elements). This odontogenic tumour can occur in two forms: a complex odontoma or a compound odontoma. Mostly these tumours occur at a young age and are usually discovered by coincidence or as tooth eruption is compromised. The diagnosis is therefore usually made around or shortly after tooth eruption, and at that time, calcification of any odontoma is already complete. Odontomas are mostly intraosseous lesions, rarely found in soft tissues, and mostly associated with the permanent dentition. Histologically, the diagnosis is made when enamel and dentine are present [2]. Radiologically, an orthopantomogram (OPG) or panoramic radiographs may help to evaluate the vertical position, level of calcification of odontomas, and impaction of deciduous or permanent teeth, and detailed occlusal radiographs can evaluate their relation to adjacent teeth. However, diagnosis on a two-dimensional image is not always straightforward. Consequently, cone beam computed tomography (CBCT) can reveal a more precise positioning, both vertically and horizontally, the composition of odontomas, root resorption, and closer relations to the adjacent teeth and cortical border [2]. CBCT is used in oral and maxillofacial surgery for its low cost, easy accessibility, and low radiation compared with multi-slice computerized tomography [3]. Therefore, the relevance of CBCT on diagnosis, the value of a classification matrix, and appropriate surgical planning of complex and compound odontomas will be discussed in this review.

Materials and methods

Search strategy

Two systematic search strings on computerized database were conducted on 2 February 2022 (classification) and 5 February 2022 (CBCT figures). The database PubMed (Medline) was used, and a search string was conducted by one observer to identify studies that included two concepts: odontomas and diagnostic imaging. Two search equations were used to build an open classification matrix for compound and complex odontoma for dentomaxillofacial CBCT radiologists. [4-22] Only full free articles accessible were included.

To find already existing classifications on odontoma, the first search equation was used: (("odontoma"[MeSH Terms] OR "odontoma"[All Fields] OR "odontomas"[All

Fields]) AND ("classification"[MeSH Terms] OR "classification"[All Fields] OR "classifications"[All Fields] OR "classification"[MeSH Subheading] OR "classification s"[All Fields] OR "classificator"[All Fields] OR "classificators"[All Fields])) AND ((ffrft[Filter]) AND (2003:2022[pdat])). The search was performed on 2 February 2022. The exclusion criteria were articles without CBCT figures of complex and/or compound odontoma, no free access to the pdf of the article, retracted articles, and articles written in other language than English or French. We included only articles with available figures of odontoma using CBCT.

To find CBCT figures of compound or complex odontoma, a second search equation was used: ("odontoma"[MeSH Terms] OR "odontoma"[All Fields] OR "odontomas"[All Fields]) AND ((ffrft[Filter]) AND (2003:2022[pdat])). The search was performed on 5 February 2022. The exclusion criteria were articles without CBCT figures of complex and/or compound odontoma, no free access to the pdf of the article, retracted articles, and articles written in other language than English or French. Only articles with available figures of odontoma using CBCT were included.

Article selection

The time period was limited from 2003 (first CBCT device accessible for dentists) to 2022. The selected languages were English and French. The inclusion criteria were free full text articles on central compound and/or complex odontoma. The exclusion criteria were experimental studies, animal studies, studies not specifically related to compound o complex odontoma. Moreover, available figures on odontoma were searched using CBCT in all selected articles.

Results

This search revealed 391 papers by reviewing the databases mentioned above. Consequently, 47 articles were found for the first search string on classification. Six articles were selected [4-9], and 41 articles were excluded. However, these 6 selected articles gave no figures of odontoma when using CBCT.
For the second search string regarding CBCT figures, 344 articles were found. After application of inclusion/exclusion criteria 13 articles were selected. Six articles (and 7 CBCT figures) were found on complex odontomas [10-15]. Seven articles (and 14 CBCT figures) were found on compound odontomas [16-22].

Finally, the construction of the open classification matrix for compound and complex odontoma for dentomaxillofacial CBCT radiologists (Table 1) was performed using 19 articles [4-22]. Both figures from literature as from our patients were included. All figures can be found as 'FIG' in this study under the subtitle 'clinical case presentation', or as 'figure' referring to an open access article with the number of the figure found in the article. Already existing classifications were used,

as well as new classifications. The new classifications from this study are marked as '[add]'. The FDI World Dental Federation (ISO) notation was used for teeth numbering.

Table 1. Open classification matrix for compound and complex odontoma for dentomaxillofacial CBCT radiologists. Open classification matrix using 19 articles for complex and compound odontomas describing: 1) Giant odontoma; 2) Quantity; 3) Location within the arch; 4) Location in relation with adjacent teeth; 5) Maxilla location; 6) Mandible location; 7) Type; 8) Complications.

	Compound odontoma	**Complex odontoma**
Giant odontoma (>3cm)		(figure 3) [14] (This study FIG 37-FIG 50)
Quantity		
Unique site	(figure 2, figure 5) [7]; (figure 3) [16]; (figure 1) [17]; (figure 6A, 6C, 6D) [18]; (figures 3-8) [20]; (figure 1) [21]; (figure 4C) [22] (This study FIG 1-FIG 25)	(figure 1, maxillary tuberosity) [10]; (figures 1, 2) [11]; (figure 1) [12]; (figure 3) [14]; (figure 1) [15]; (figure 6B) [18] (This study FIG 26-FIG 32)
Multiple sites	(This study FIG 33-FIG 35)	(figure 3) [13]
Location within the arch [4]		
Intraosseous [9]	(figure 3) [16]; (figure 1) [17]; (figure 6A, 6C, 6D) [18]; (figure 2, figure 5) [19]; (figures 3-8) [20]; (figure 1) [21]; (figure 4C) [22] (This study FIG 1-FIG 19, FIG 21-FIG 25, FIG 33-FIG 36)	(figure 1, maxillary tuberosity) [10]; (figures 1, 2) [11]; (figure 1) [12]; (figure 1) [15]; (figure 6B) [18] (This study FIG 26-FIG 32)
[add] Pre-erupted state (perforation of alveolar bone on the dental arch)	(This study FIG 20, FIG 33, FIG 34, FIG 36)	
Erupted [9]		(figure 3) [13]; (figure 3) [14] (This study FIG 38-FIG 40, FIG 42, FIG 45-FIG 48)
Extragnathic		(This study FIG 37-FIG

		50)
[add] Partially extragnathic	(This study FIG 33, FIG 34, FIG 36)	(This study FIG 26, FIG 27)
Location in relation with adjacent teeth		
Inside and/or[add] between deciduous tooth roots and above definitive tooth [23]	(figure 3) [16]; (figure 1) [17]; (figure 6A) [18]; (figure 1, figure 4C) [22] (This study FIG 1, FIG 3, FIG 4, FIG 15, FIG 16, FIG 18)	
Lateral to deciduous tooth [23]		
In dentigerous cyst which is occlusal to deciduous tooth [23]	(figures 3-8) [20]	
Inside follicle surrounding deciduous tooth [23]		
Around the root/roots of the deciduous tooth [23]	(This study FIG 15)	
[add] Occlusal to the definitive teeth	(figure 1) [21] (This study FIG 1, FIG 3, FIG 4, FIG 15, FIG 16, FIG 22, FIG 25, FIG 33-FIG 35)	(figures 1, 2) [11]; (figure 3) [13]
[add] Around the crown of the definitive tooth	(This study FIG 34)	(figure 1) [12]; (figure 6B) [18]
[add] Around the root of the definitive tooth	(figure 6C, 6D) [18] (This study FIG 11-FIG 14, FIG 33-FIG 35	(figure 1) [15] (This study FIG 30)
[add] Lateral to definitive teeth	(figure 2, figure 5) [19] (This study FIG 2-FIG 6, FIG 8-FIG 10, FIG 17, FIG 21-FIG 25, FIG 33-FIG 35)	
[add] Replacement of definitive teeth	(This study FIG 19, FIG 20, FIG 22-FIG 24)	(figure 3) [14]
[add] Distal to last tooth on the arch		(figure 1, maxillary tuberosity) [10]
[add] Apical to apices of teeth		(This study FIG 26, FIG 28, FIG 29)
[add] Maxilla location		
Anterior (teeth 13-23) [5-7, 9]	(figure 3) [16]; (figure 6A, 6C) [18]; (figure 1) [21]; (figure 4C) [22]	(figure 1) [15]; (figure 6B) [18]

	(This study FIG 1-FIG 4)	
Premolar (teeth 15-13, 25-23)	(figure 1) [17]; (figure 6D) [18]; (figures 3-8) [20] (This study FIG 5-FIG 7, FIG 33-FIG 35)	(This study FIG 26, FIG 42, FIG 45-FIG 48)
Molars (teeth 18-16, 28-26)	(This study FIG 33-FIG 35)	(figure 1, maxillary tuberosity) [10]; (figures 1, 2) [11]; (figure 1) [12] (This study FIG 42, FIG 45-FIG 48)
[add] Mandible location		
Anterior (teeth 43-33)	(This study FIG 8-FIG 25)	(figure 6B) [18] (This study FIG 28, FIG 29)
Premolar (teeth 45-43, 35-33)	(figure 2, figure 5) [19]	(figure 3) [14]
Molar (teeth 48-46, 38-36) [5-7, 9]		(figure 3) [13]; (figure 3) [14] (This study FIG 30)
Type [4]		
Denticulo- type [4, 6]	(figure 1) [17]; (figure 2, figure 5) [19]; (figure 4C) [22] (This study FIG 1-FIG 4, FIG 19-FIG 21, FIG 33-FIG 36)	
Particle type [4]	(figures 3-8) [20]; (figure 1) [21] (This study FIG 5-FIG 7, FIG 11-FIG 14)	
Denticulo-particle type [4]	(figure 3) [16] (This study FIG 8-FIG 10)	
[add] denticulo-amorphous type	(This study FIG 15, FIG 18, FIG 22-FIG 25)	(This study FIG 42, FIG 43, FIG 45-FIG 48, FIG 50)
Amorphous tissue [4]	(This study FIG 15, FIG 17, FIG 25)	(figure 1, maxillary tuberosity) [10]; (figures 1, 2) [11]; (figure 1) [12]; (figure 3) [14]; (figure 3)

		[13]; (figure 1) [15] (This study FIG 26-FIG 30, FIG 32, FIG 37-FIG 44, FIG 49)
Complications		
[add] Adjacent deciduous teeth resorption	(This study FIG 1, FIG 3, FIG 4)	
[add] Adjacent definitive teeth resorption	(This study FIG 5, FIG 6, FIG 16, FIG 21, FIG 33, FIG 34)	(figure 1) [15] (This study FIG 30, FIG 45)
[add] Relationship with inferior alveolar nerve or with other cranial nerves		(This study FIG 31, FIG 32, FIG 38-FIG 41, FIG 46, FIG 47)
Deciduous teeth retention [4, 6, 7, 9]	(figures 3-8) [20]	
Definitive teeth retention/impaction [6, 7, 9]	(figure 3) [16]; (figures 3-8) [20]; (figure 1) [21] (This study FIG 1, FIG 3, FIG 4, FIG 15, FIG 16, FIG 18, FIG 19, FIG 22, FIG 25, FIG 33-FIG 35)	Displacement of tooth 18 (figures 1, 2) [11]
Displacement of teeth/malposition [4, 9]/[add] rotation/diastema between teeth	(figure 1) [17]; (figures 3-8) [20] (This study FIG 11, FIG 12, FIG 14)	Displacement of tooth 18 (figures 1, 2) [11]; Displacement of tooth 45 (figure 3) [14]
Transmigration of teeth	(This study FIG 15, FIG 16, FIG 18, FIG 22, FIG 25)	
Bony expansion [4, 6]	(This study FIG 16, FIG 17, FIG 24)	
[add] thinning of vestibular/buccal cortical bone related to the odontoma	(This study FIG 1, FIG 16, FIG 20, FIG 21, FIG 24)	(This study FIG 29, FIG 31)
[add] perforation of vestibular/buccal cortical bone related to the odontoma		
[add] thinning of lingual/palatine cortical bone related to the odontoma	(This study FIG 6, FIG 7, FIG 16, FIG 20, FIG 24, FIG 34)	(This study FIG 32)
[add] perforation of lingual/palatine cortical bone related to the odontoma	(This study FIG 9)	
Mouth opening limitation [10]		(figure 1) [10]

Delayed root formation [12]		(figure 1) [12]
[add] Fusion between odontoma and follicular sac of adjacent impacted tooth	(This study FIG 1, FIG 2)	
[add] Oro-antral fistula/communication		(This study FIG 39, FIG 45-FIG 48)
[add] Maxillary sinus expansion		(This study FIG 40)
[add] Hyperostosis of maxillary sinus walls		(This study FIG 39, FIG 40, FIG 43-FIG 48)
[add] Thinning/erosion of maxillary sinus walls		(This study FIG 41, FIG 43)
[add] Perforation of maxillary sinus walls		(This study FIG 42, FIG 44, FIG 46-FIG 48)

Clinical cases presentation for compound odontoma

Maxilla, denticulo-type in canine area

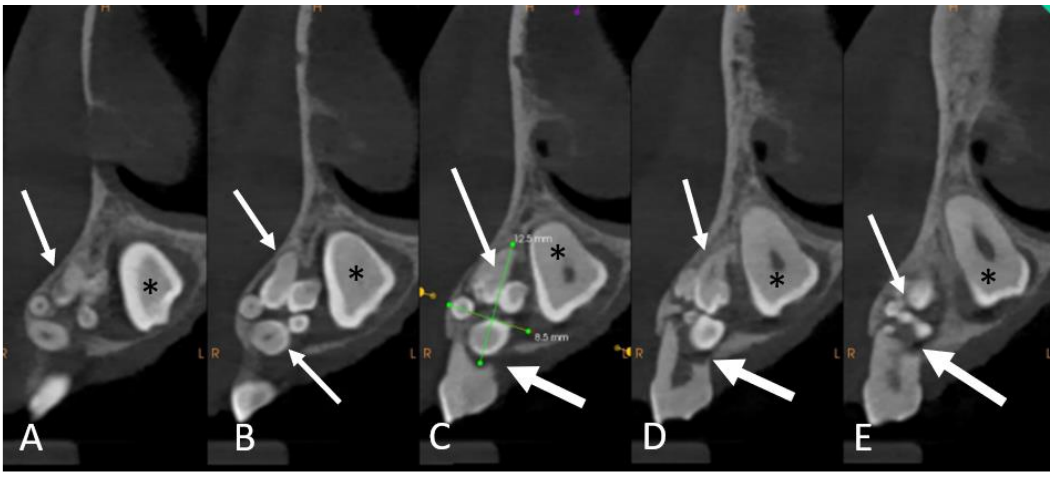

Fig. 1. Patient n°1. (Patient 14 years-old). Carestream 9600 CBCT. A-E: Multi-reformatted coronal view. * Impacted tooth n°13. A-E: small arrow: denticulo-type compound odontoma situated between deciduous tooth n°53 and impacted tooth n°13. C-E: thick arrow: external resorption of the tooth n°83 by the odontoma. B-D: association of the odontoma with the follicular sac surrounding the crown of the tooth n°13. C, D: thinning of the vestibular cortical bone by the odontoma.

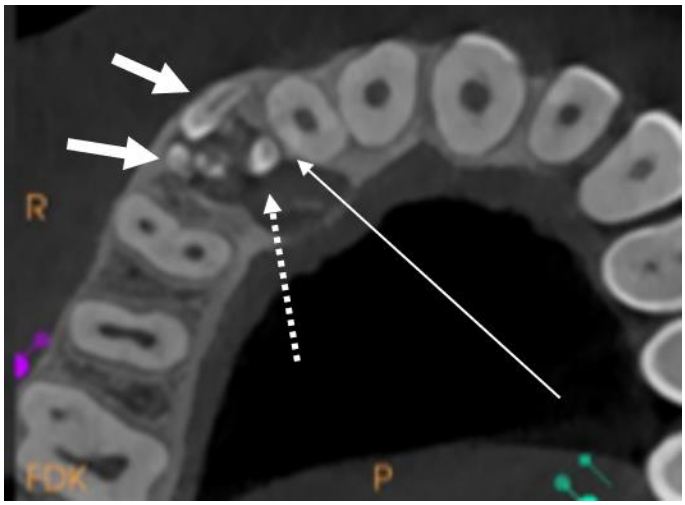

Fig. 2. Patient n°1. (Patient 14 years-old). Carestream 9600 CBCT. Axial view. Thick arrows: denticulo-type compound odontoma thinning the vestibular cortical bone. Dotted arrow: fusion between the odontoma and the follicular sac of the tooth n°13. Thin arrow: close contact between the odontoma and the root of the tooth n°12, without external resorption.

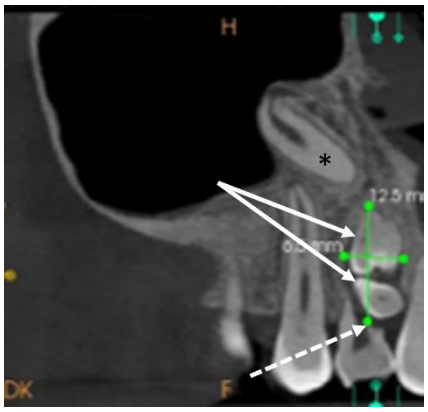

Fig. 3. Patient n°1. (Patient 14 years-old). Carestream 9600 CBCT. Multi-reformatted sagittal view. Arrows: denticulo-type compound odontoma between tooth n°53 and tooth n°13 (*). Discontinuous arrow: external resorption of the tooth n°53 by the odontoma. Tooth n°13(*) has a hooked apex and is surrounded by the right maxillary sinus.

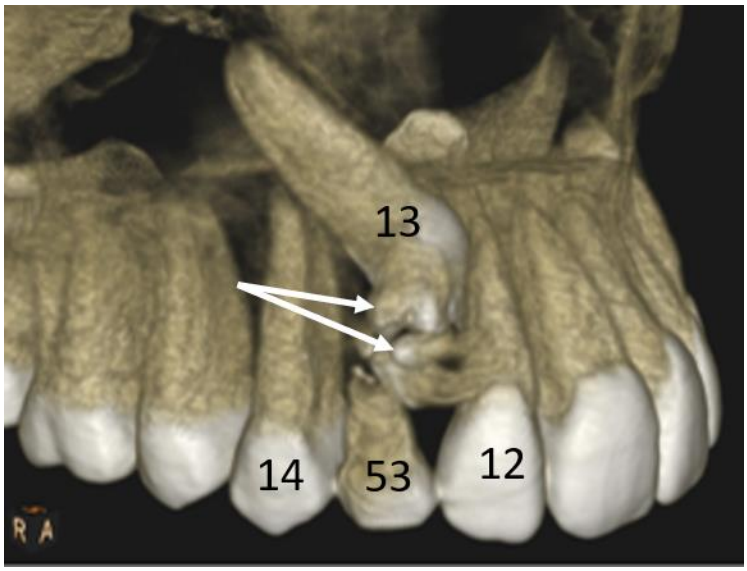

Fig. 4. Patient n°1. (Patient 14 years-old). Carestream 9600 CBCT. 3D reconstruction view. Arrows: denticulo-type compound odontoma between tooth n°53 and tooth n°13.

Maxilla, particle-type in premolar area

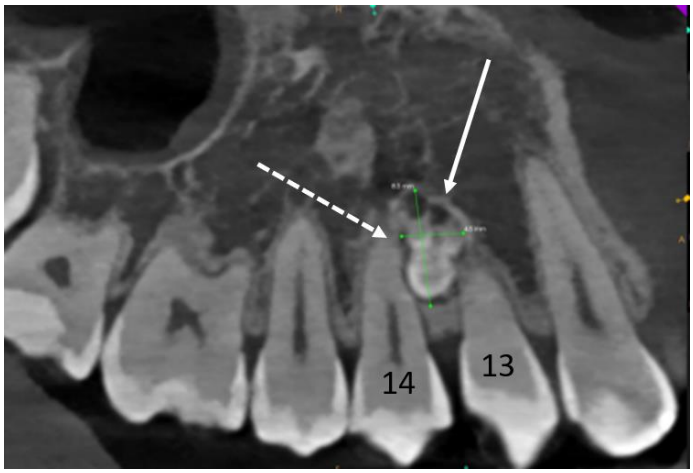

Fig. 5. Patient n°2. (Patient 20 years-old). Carestream 9600 CBCT. Multi-reformatted sagittal view. Arrow: particle-type compound odontoma between the roots of teeth n°13 and n°14. Discontinuous arrow: discrete external resorption of the apical and mesial side of the root of the tooth n°14. Diastema between crowns of teeth n°13 and n°14.

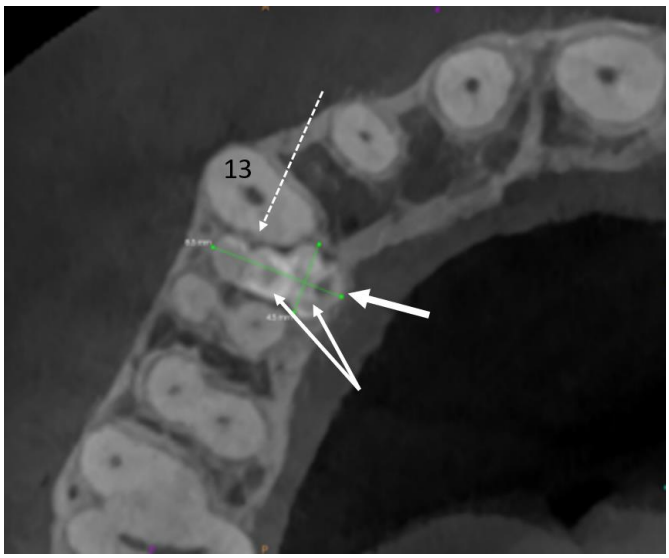

Fig. 6. Patient n°2. (Patient 20 years-old). Carestream 9600 CBCT. Axial view. Thin arrows: particle-type compound odontoma situated between roots of teeth n°13 and n°14. Thick arrow: thinning of the palatine cortical bone by the odontoma. Thin discontinuous arrow: discrete external resorption of the distal side of the root of the tooth n°13.

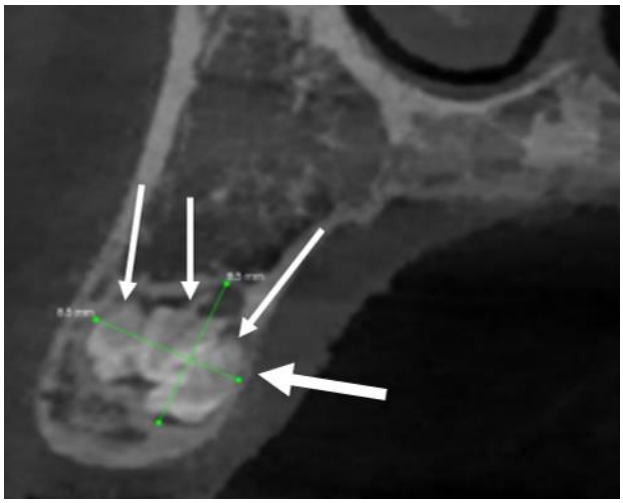

Fig. 7. Patient n°2. (Patient 20 years-old). Carestream 9600 CBCT. Coronal view. Arrows: particle-type compound odontoma. Thick arrow: thinning of the palatine cortical bone by the odontoma.

Mandible, denticulo-particle type in anterior area

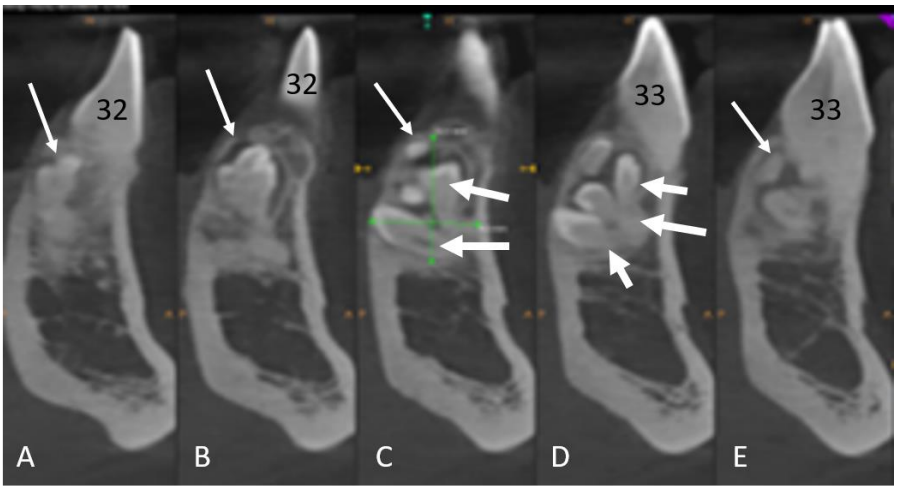

Fig. 8. Patient n°3. (Patient 39 years–old). Carestream 9600 CBCT. Multi-reformatted coronal view. A-E: denticulo-particle type compound odontoma positioned between roots of teeth n°32 and n°33. A-C, E: Thin arrows: particle-type component. C, D: thick arrows: denticulo-type component.

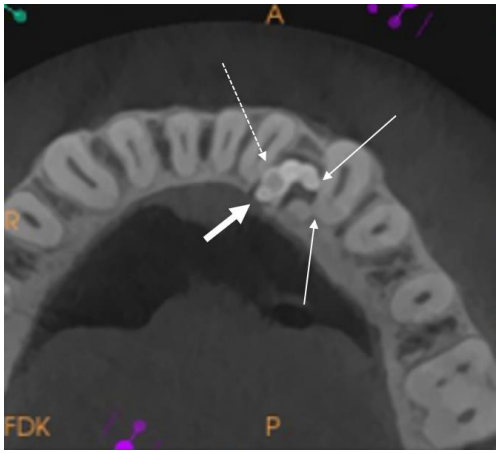

Fig. 9. Patient n°3. (Patient 39 years–old). Carestream 9600 CBCT. Axial view. Compound odontoma between teeth n°32 and n°33. Thin discontinuous arrow: close contact without external resorption between the odontoma and the distal side of the root of the tooth n°32. Thin arrow: close contact without external resorption between the odontoma and the mesial side of the root of the tooth n°33. Thick arrow: perforation of the lingual cortical bone by the odontoma.

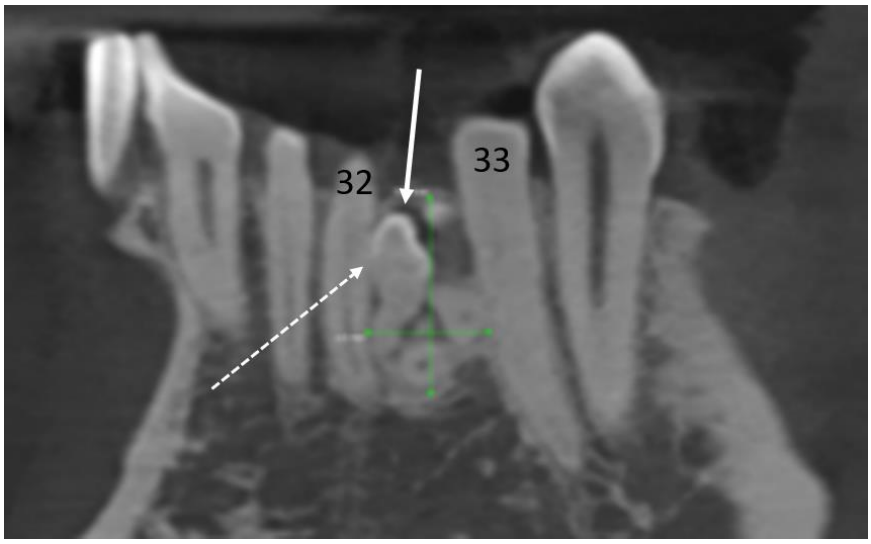

Fig. 10. Patient n°3. (Patient 39 years–old). Carestream 9600 CBCT. Multi-reformatted sagittal view. Arrow: compound odontoma between teeth n°32 and 33. Discontinuous arrow: close contact between the odontoma (denticulo-particle type compound), and the distal side of the root of the tooth n°32.

Mandible, particle-type in anterior area, lingual to canine

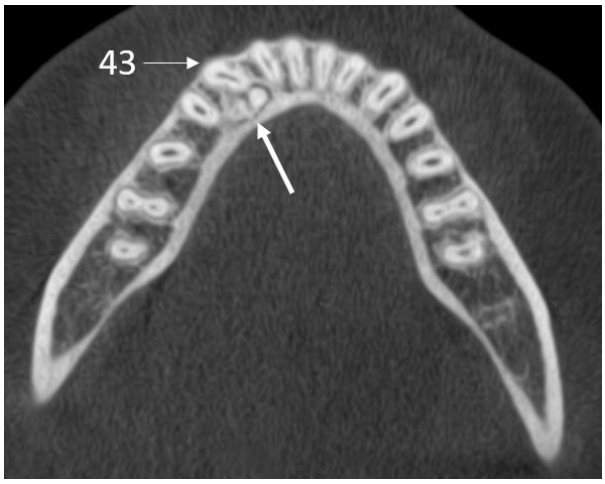

Fig. 11. Patient n°4. (Patient 14 years-old). Planmeca 3D Mid. Axial view. Arrow: particle-type compound odontoma on the lingual and distal side of the root of the tooth n°43. Tooth n°43 is in rotation with its mesial face turned toward vestibular side.

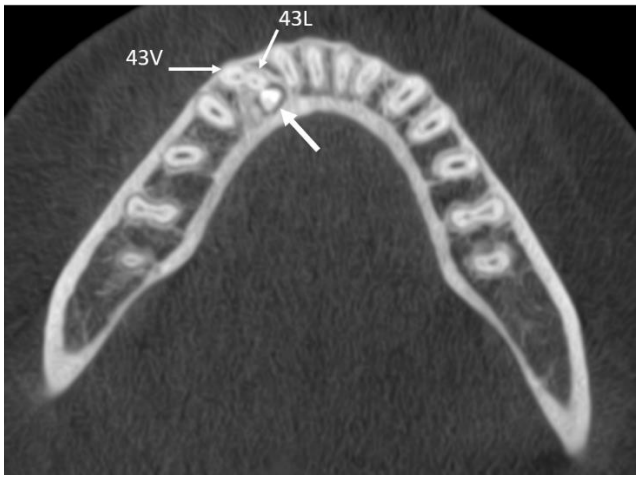

Fig. 12. Patient n°4. (Patient 14 years-old). Planmeca 3D Mid. Axial view. Arrow: particle-type compound odontoma on the lingual side of the root of the tooth n°43. Tooth n°43 presents with two roots: vestibular and lingual. Close contact without external resorption between the odontoma and the lingual root of the tooth n°43.

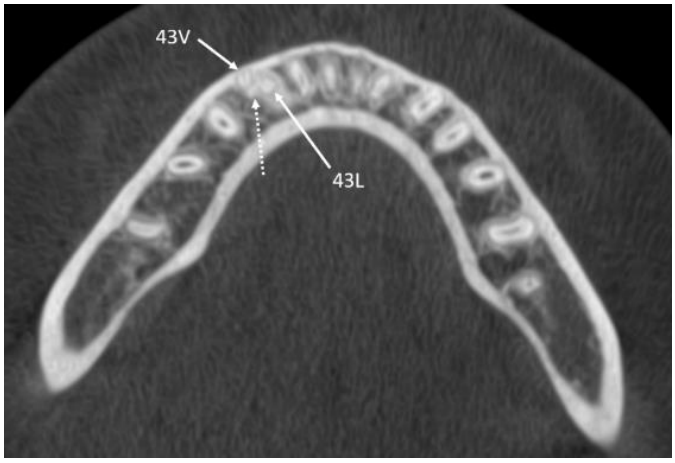

Fig. 13. Patient n°4. (Patient 14 years-old). Planmeca 3D Mid. Axial view. Dotted arrow: particle-type odontoma between the lingual and the vestibular root of the tooth n°43.

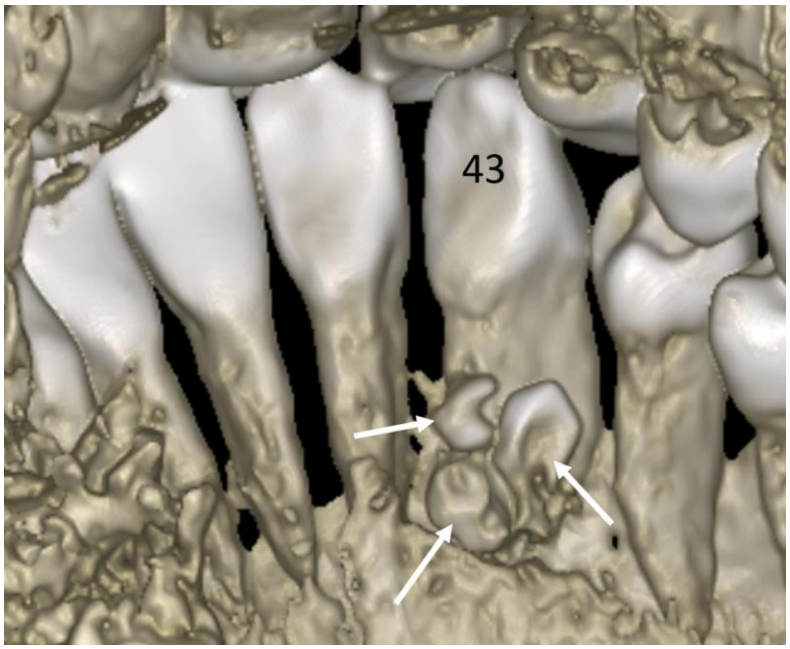

Fig. 14. Patient n°4. (Patient 14 years-old). Planmeca 3D Mid. 3D reconstruction view. Arrows: particle-type compound odontoma on the lingual side of the root of the tooth n°43. Rotation of the tooth n°43 with its mesial side turned toward vestibular side. Diastema between the crowns of teeth n°42 and n°43.

Mandible, denticulo-amorphous type in anterior area

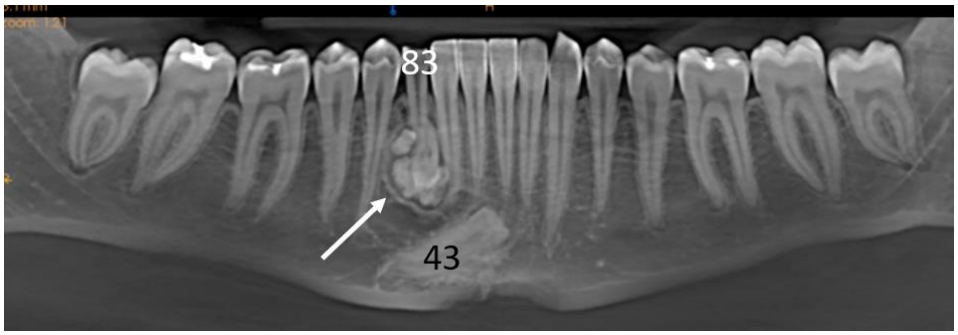

Fig. 15. Patient n°5. (Patient 19 years-old). Carestream 9600 CBCT. Pseudopanoramic reformatted view. Arrow: denticulo-amorphous type odontoma between the tooth n°83 and impacted tooth n°43. The tooth n°43 is in transmigration under the apices of roots of teeth n°41 and n°31.

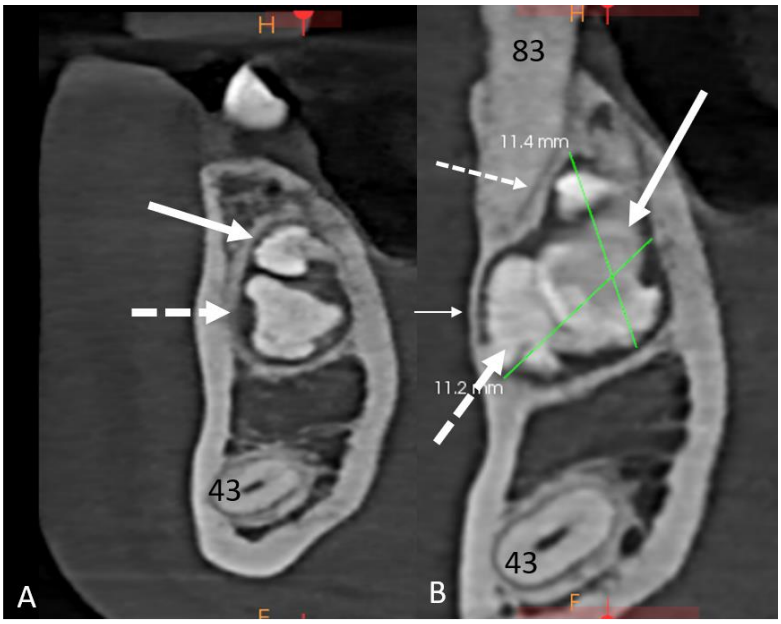

Fig. 16. Patient n°5. (Patient 19 years-old). Carestream 9600 CBCT. Multi-reformatted coronal view through the odontoma. A. Arrow: denticule content of the odontoma. Discontinued arrow: amorphous content of the odontoma. Tooth n°43 is situated close to the basilar cortex of the mandible. B. Thick arrow: denticule content of the odontoma with malformed crown directed inferiorly. Discontinuous thick arrow: amorphous content of the odontoma. Thin arrow: bony expansion and thinning of the vestibular cortex. Thin discontinuous arrow: external resorption of the root of the tooth n°83 by the odontoma. Presence of thinning of the lingual cortical bone by the odontoma lingual to the tooth n°83.

Fig. 17. Patient n°5. (Patient 19 years-old). Carestream 9600 CBCT. Axial view. Discontinuous arrow: amorphous content of the odontoma. Thin arrow: vestibular bony expansion and thinning of the vestibular cortex. Thin discontinuous arrow: odontoma surrounding the root of the tooth n°42 without its external root resorption.

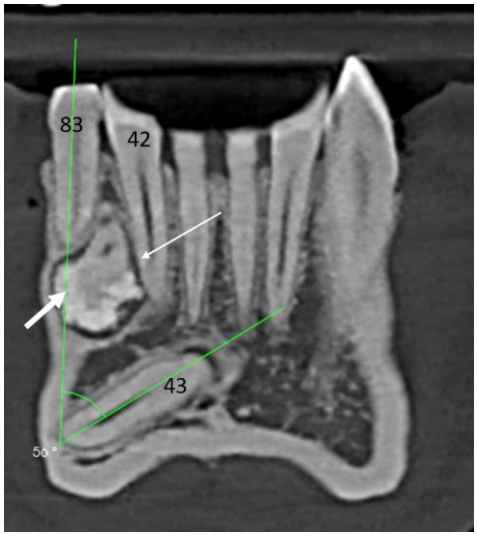

Fig. 18. Patient n°5. (Patient 19 years-old). Carestream 9600 CBCT. Multi-reformatted coronal view. Thick arrow: denticulo-amorphous type odontoma between the roots of the teeth n°83 and n°42. Thin arrow: close relationship between the odontoma and the distal side of the root of the tooth n°42. Impacted tooth n°43 in transmigration, without ankylosis, and at a distance from the apex of the root of the tooth n°41.

287 **Mandible, denticulo-type in anterior area, impaction of canine**

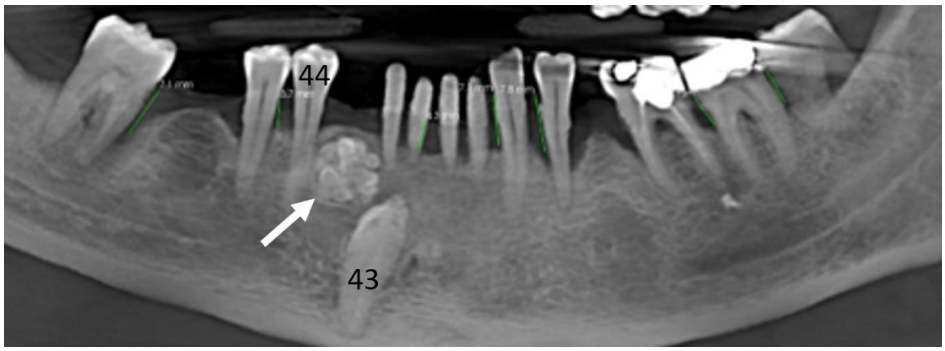

288
289 **Fig. 19. Patient n°6. (Patient 64 years-old).** Carestream 9600 CBCT.
290 Pseudopanoramic reformatted view. Arrow: Denticulo-type odontoma
291 between the roots of the teeth n°44 and n°42. Tooth n°43 impacted and
292 vertical without transmigration.
293

294
295 **Fig. 20. Patient n°6. (Patient 64 years-old).** Carestream 9600 CBCT. Multi-
296 reformatted coronal view. Thin arrow: thinning of the vestibular cortical bone
297 by the odontoma. Discontinuous arrow: thinning of the lingual cortical bone
298 by the odontoma. Thick arrow: perforation of the alveolar bone, and pre-
299 erupted state of the odontoma.
300

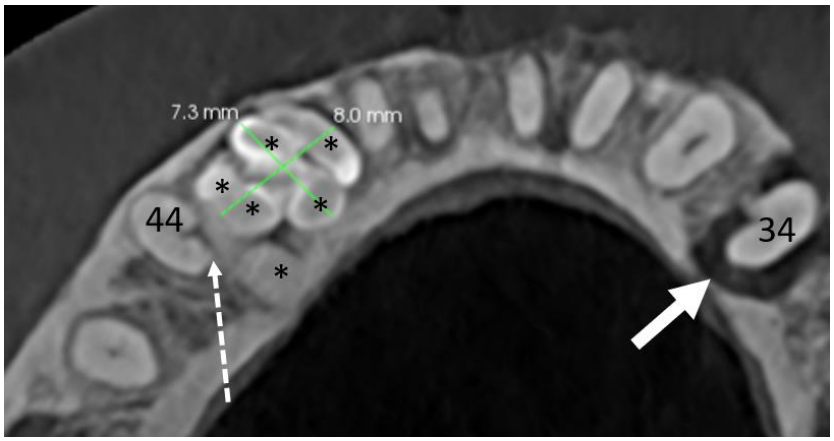

Fig. 21. Patient n°6. (Patient 64 years-old). Carestream 9600 CBCT. Axial view. Denticulo-type odontoma with multiple denticules (*). Discontinuous arrow: external resorption of the mesial side of the tooth n°44 by the odontoma. Thick arrow: advanced periodontitis around the tooth n°34.

Mandible, denticulo-amorphous type in anterior area, transmigration of canine

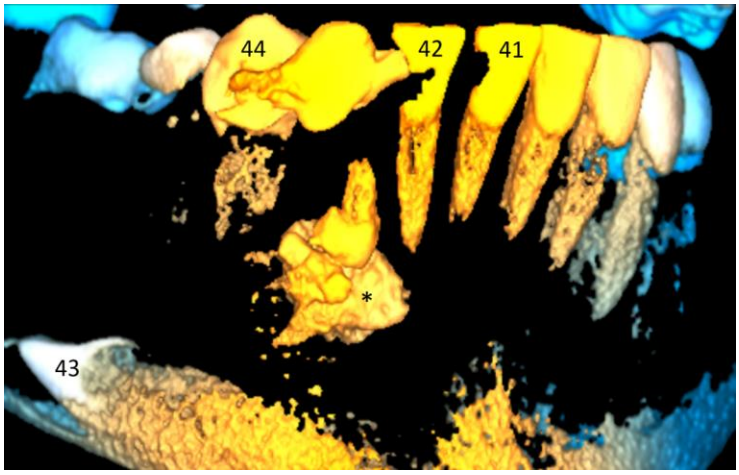

Fig. 22. Patient n°7. (Patient 23 years-old). Planmeca 3D mid. 3D reconstruction right lateral view of the mandible with threshold selecting dental tissue. Denticulo-amorphous type odontoma (*) between the teeth n°42 and n°44. Tooth n°43 in transmigration along the basilar cortical bone, and with the crown directed toward posterior. Tooth n°43 is replaced on the dental arch by the metallic prosthetic element.

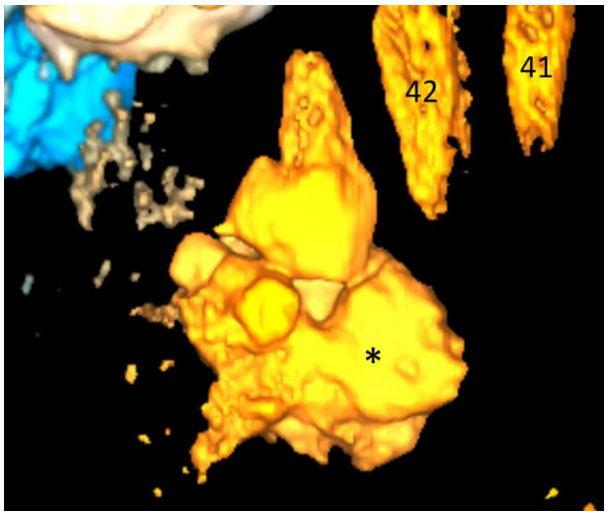

316
317 **Fig. 23. Patient n°7. (Patient 23 years-old).** Planmeca 3D mid. 3D
318 reconstruction right lateral view of the mandible. Denticulo-amorphous type
319 odontoma (*) with one of the denticules in inverted position with the crown
320 directed inferiorly.
321

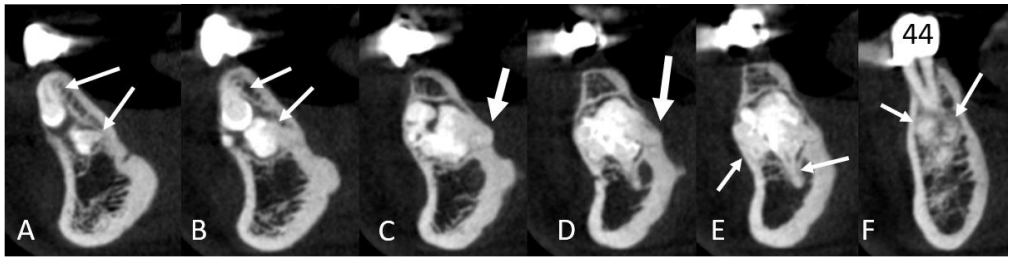

322
323 **Fig. 24. Patient n°7. (Patient 23 years-old).** Planmeca 3D mid. A-F: sagittal
324 view. A, B. Arrows: inverted and horizontal denticule. C, D. Thick arrow:
325 bone expansion of the odontoma to the lingual side. E. Thinning of the
326 vestibular cortical bone by the odontoma, and extension of the odontoma
327 inferiorly. F. Close relationship between the odontoma and the apex of the
328 root of the tooth n°44.

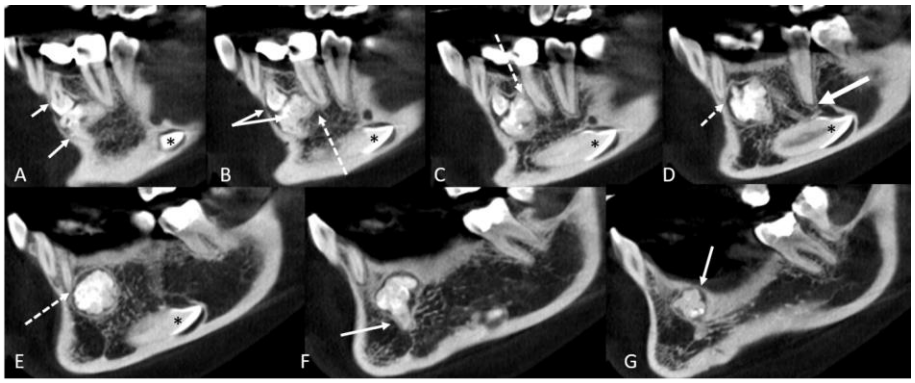

Fig. 25. Patient n°7. (Patient 23 years-old). Planmeca 3D mid. A-G: para-sagittal multi-reformatted view from vestibular (A) to lingual (G) side of the right mandible. (*) The tooth n°43 in transmigration along the basilar cortical bone. A, B. Arrows: odontoma. B, C. Discontinuous arrow: close relationship between the root of the tooth n°44 and the odonoma, and without external resorption. D, E. Discontinuous arrow: close relationship between the root of the tooth n°42 and the odontoma. D. Thick arrow: close relationship between follicular sac of the tooth n°43 and the apex of the tooth n°45. E. Presence of massive enamel component of the odontoma. F. Arrow: inferior extension of the odontoma. G. Arrow: amorphous component of the odontoma.

Clinical cases presentation for complex odontoma

Anterior maxilla

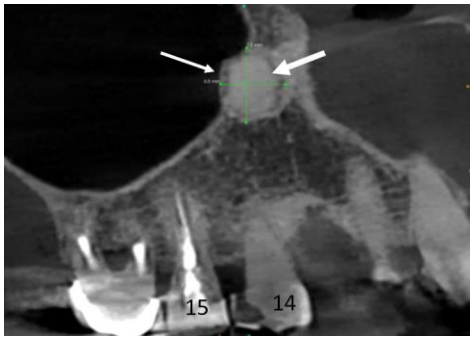

Fig. 26. Patient n°8. (Patient 64 years-old). Carestream 9600 CBCT. Multi-reformatted sagittal view. Complex odontoma in the palatine process of the right maxilla. The odontoma is situated apical to the tooth n°13. Partial extension of the complex odontoma in right maxillary sinus (partial extragnathic type).

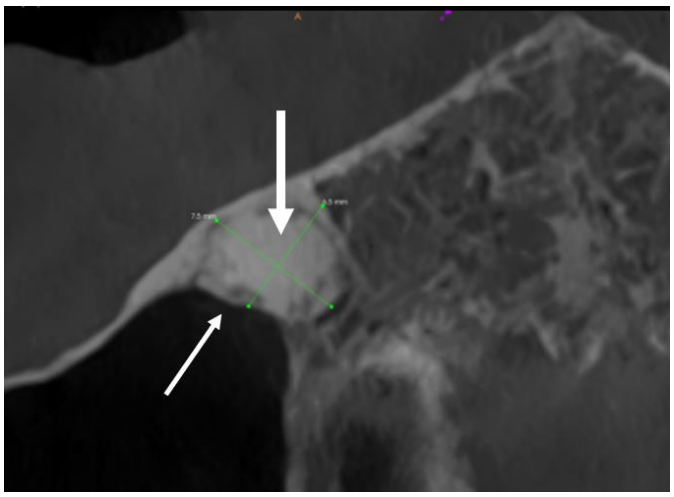

Fig. 27. Patient n°8. (Patient 64 years-old). Carestream 9600 CBCT. Axial view. Arrow: complex odontoma. Thin arrow: extension of the complex odontoma in right maxillary sinus.

Anterior mandible

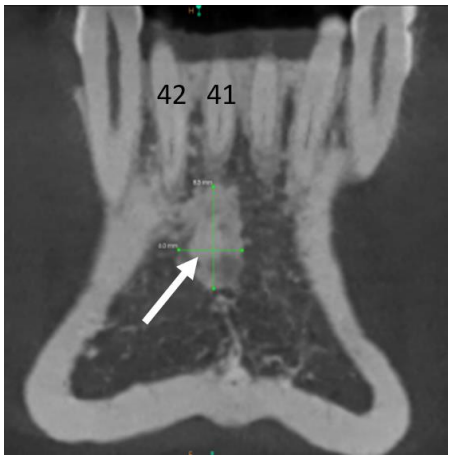

Fig. 28. Patient n°9. (Patient 43 years-old). Carestream 9600 CBCT. Multi-reformatted coronal view. Arrow: complex odontoma with close relationship with the apices of the teeth n°41, and n°42.

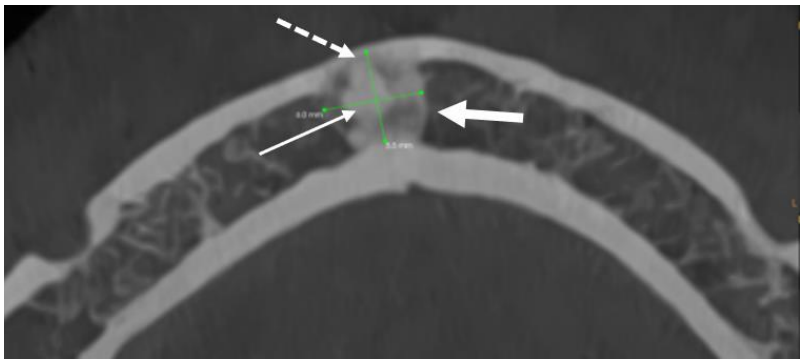

Fig. 29. Patient n°9. (Patient 43 years-old). Carestream 9600 CBCT. Axial view. Thick arrow: complex odontoma between the lingual and vestibular cortical bone in the midsagittal mandibular area. Thin arrow: amorphous component of the complex odontoma. Discontinuous arrow: thinning of the vestibular bone by the odontoma.

Posterior mandible

Fig. 30. Patient n°10. (Patient 27 years-old). Carestream 9600 CBCT. Multi-reformatted sagittal view. Thick arrow: complex odontoma close to the apex of the root of the tooth n°37. Thin arrow: external resorption of the root of the tooth n°37 by the odontoma.

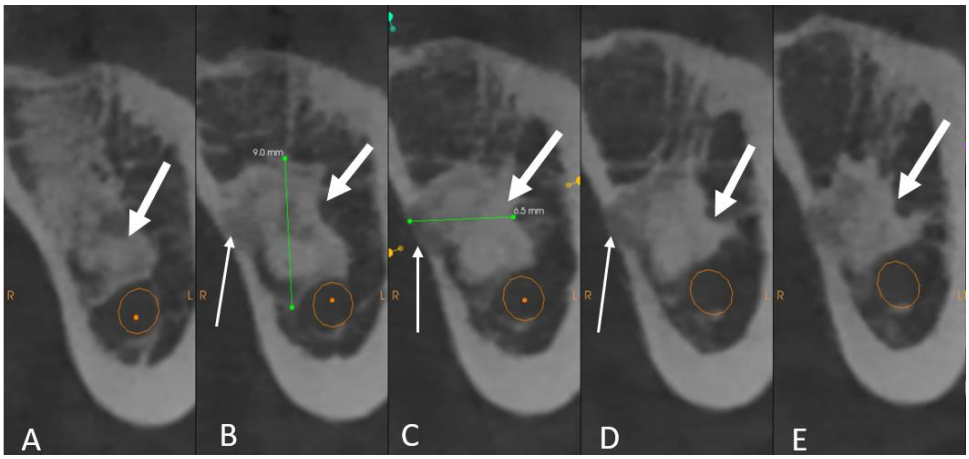

Fig. 31. Patient n°10. (Patient 27 years-old). Carestream 9600 CBCT. Multi-reformatted coronal view. A-E. Thick arrow: intra-osseous complex odontoma superior to the left inferior alveolar nerve canal (segmented with orange circle). B-D. Thin arrow: thinning of the vestibular cortical bone by the odontoma.

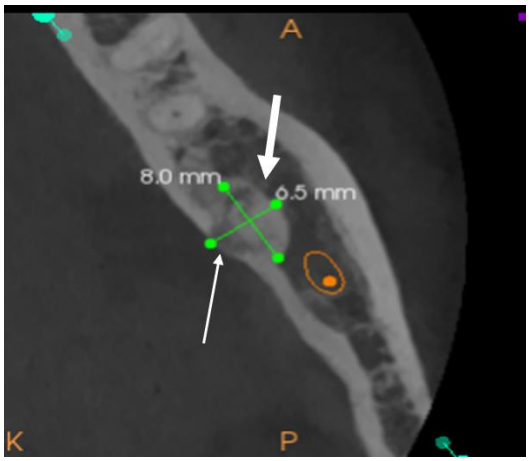

Fig. 32. Patient n°10. (Patient 27 years-old). Carestream 9600 CBCT. Axial view. Thick arrow: complex odontoma positioned close to the lingual side. Thin arrow: thinning of the lingual cortical bone by the odontoma.

Clinical cases presentation in specific situations

Multiple compound odontoma

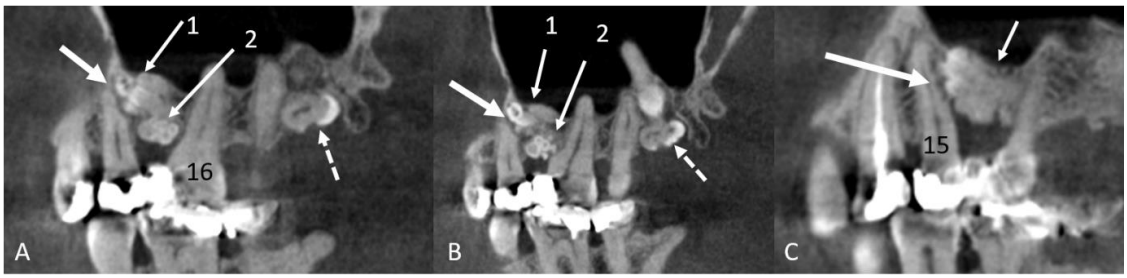

Fig. 33. Patient n°11. (Patient 43 years-old). Planmeca 3D Mid. Sagittal view of the right maxilla. A, B. 1. Upper situated denticulo-type compound odontoma between the teeth n°15 and n°16. 2. Lower situated denticulo-type compound odontoma between the teeth n°15 and n°16. Thick arrow: external resorption of the distal side of the tooth n°15. Discontinuous arrow: denticulo-type compound odontoma distal to the tooth n°17 in pre-erupted state. B. Discontinuous arrow: denticulo-type compound odontoma distal to the tooth n°17 in erupted state, and presence of impacted tooth n°18 with its root surrounded by the right maxillary sinus. C. Upper denticulo-type compound odontoma at the floor of the right maxillary sinus. Thick arrow: external resorption of the distal side of the tooth n°15 by the upper situated odontoma.

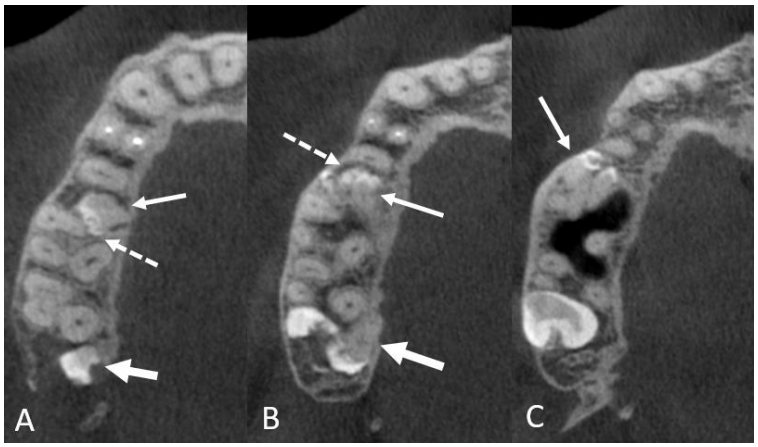

Fig. 34. Patient n°11. (Patient 43 years-old). Planmeca 3D Mid. Axial view. A. Arrow: lower situated denticulo-type compound odontoma between the teeth n°15 and n°16. Discontinuous arrow: external resorption of the mesio-vestibular root of the tooth n°16 by the lower situated denticulo-type compound odontoma. Thick arrow: denticulo-type compound odontoma distal and palatine to the tooth n°17, and in pre-erupted state. B. Arrow: Upper situated denticulo-type compound odontoma between the teeth n°15 and n°16. Discontinuous arrow: external resorption of the distal side of the root of the tooth n°15 by the upper situated denticulo-type compound odontoma. Thick arrow: denticulo-type compound odontoma distal and palatine to the tooth n°17, and palatine to the crown of the tooth n°18. C. Arrow: upper situated denticulo-type compound odontoma with close relationship with the right maxillary sinus.

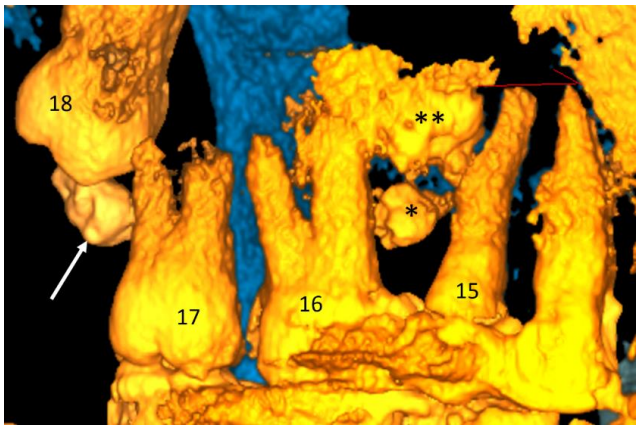

Fig. 35. Patient n°11. (Patient 43 years-old). Planmeca 3D Mid. 3D reconstruction view of the right lateral maxilla. (*) lower situated denticulo-type compound odontoma, (**) upper situated denticulo-type compound odontoma. Arrow: denticulo-type compound odontoma distal to the roots of the tooth n°17, and apical to the crown of the tooth n°18.

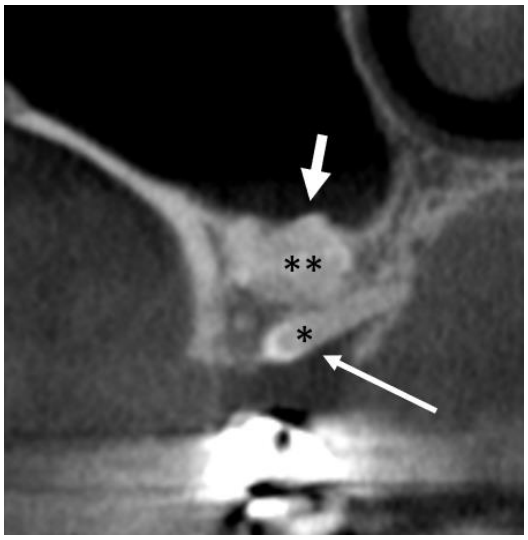

Fig. 36. Patient n°11. (Patient 43 years-old). Planmeca 3D Mid. Coronal view. (*) lower situated denticulo-type compound odontoma, (**) upper situated denticulo-type compound odontoma. Arrow: lower situated denticulo-type compound odontoma is in pre-eruptive state. Thick arrow: (**) upper situated denticulo-type compound odontoma at the floor of the right maxillary sinus.

440 **Double extragnathic complex odontoma**

441
442 **Fig. 37. Patient n°12. (Patient 69 years-old).** Planmeca 3D Mid. Coronal
443 view of the anterior maxillary sinus. (*) Anterior complex odontoma inside the
444 left maxillary sinus. Arrow: amorphous tissue component of the complex
445 odontoma. Discontinuous arrow: denticule tissue component of the complex
446 odontoma.
447
448
449

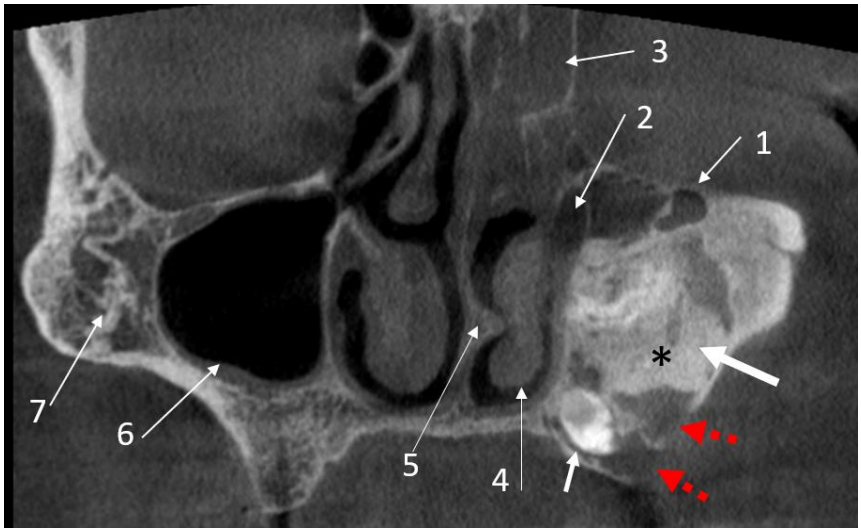

Fig. 38. Patient n°12. (Patient 69 years-old). Planmeca 3D Mid. Coronal view of the midsection of the anterior complex odontoma (*). Thick arrow: amorphous tissue component of the complex odontoma. Arrow: denticule tissue component of the complex odontoma in the palatine process of the left maxilla. Red arrows: perforations of the lateral wall of the left maxilla by the expansion and eruption of the odontoma. 1. Left suborbital nerve canal surrounded by the complex odontoma. 2. Close relationship between complex odontoma and the left nasolacrimal duct. 3. Thickening of the mucosa around the left middle turbinate and in the left ethmoid sinus cells. 4. Paradoxal left inferior turbinate. 5. Bone spur from nasal septum directed toward left, and in contact with the left inferior turbinate. 6. Discrete thickening of the mucosa in the right maxillary sinus. 7. Right zygomatico-maxillary suture.

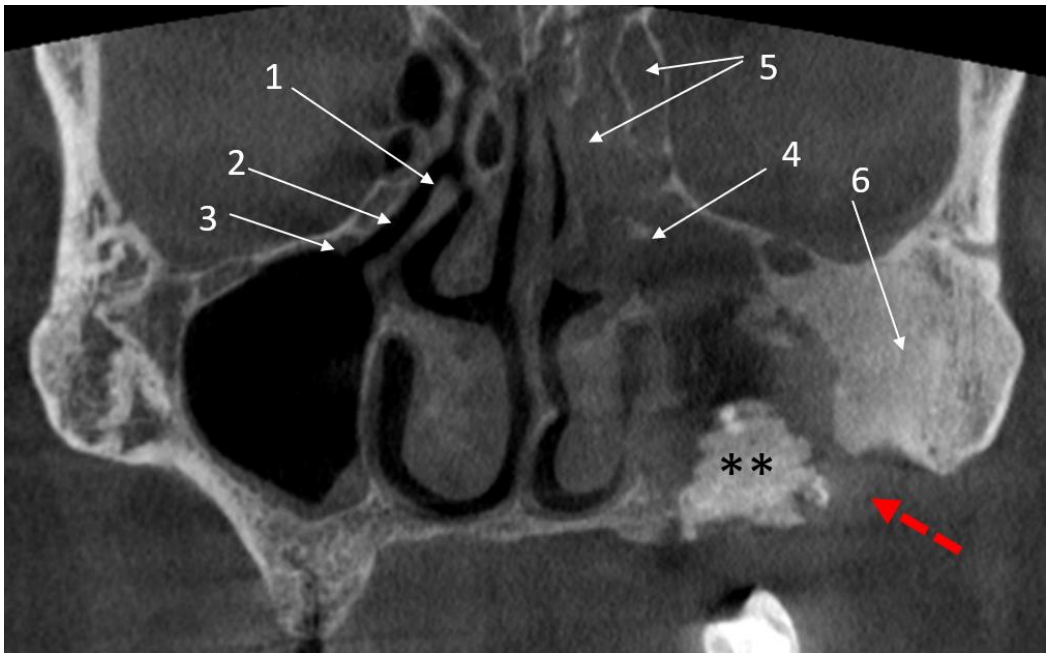

Fig. 39. Patient n°12. (Patient 69 years-old). Planmeca 3D Mid. Coronal view of the intermediate area between anterior and posterior complex odontoma (**). Red discontinuous arrow: perforation at the level of the left alveolar bone, and presence of major oro-sinusal fistula. 1. Right unicinate process. 2. Right infundibulum. 3. Right ostium. 4. Absence of left unicinate process, of left infundibulum, and of left ostium. 5. Thickening of the mucosa around the left middle turbinate and in the left ethmoid sinus cells. 6. Hyperostosis of the left zygomaticomaxillary process. Left suborbital nerve canal surrounded by the complex odontoma.

Fig. 40. Patient n°12. (Patient 69 years-old). Planmeca 3D Mid. Coronal view of the midsection of the posterior complex odontoma (**). Red discontinuous arrow: perforation of the left alveolar bone, and the complex odontoma in eruptive state. Arrow: posterior complex odontoma (**) with amorphous tissue content. 1. Thickening and internal erosion of the left lateral wall of the left maxillary sinus. 2. Thickening of the floor of the left orbit. 3. Thickening of the nasal wall of the left maxillary sinus. 4. Thickening of the mucosa and in the posterior cells of the left ethmoid sinus. 5. Thickening of the mucosa around the left middle turbinate. 6. Transverse expansion of the maxillary sinus due to the presence of the complex odontoma. 7. Decreasing in transversal dimension of the left nasal fossa.

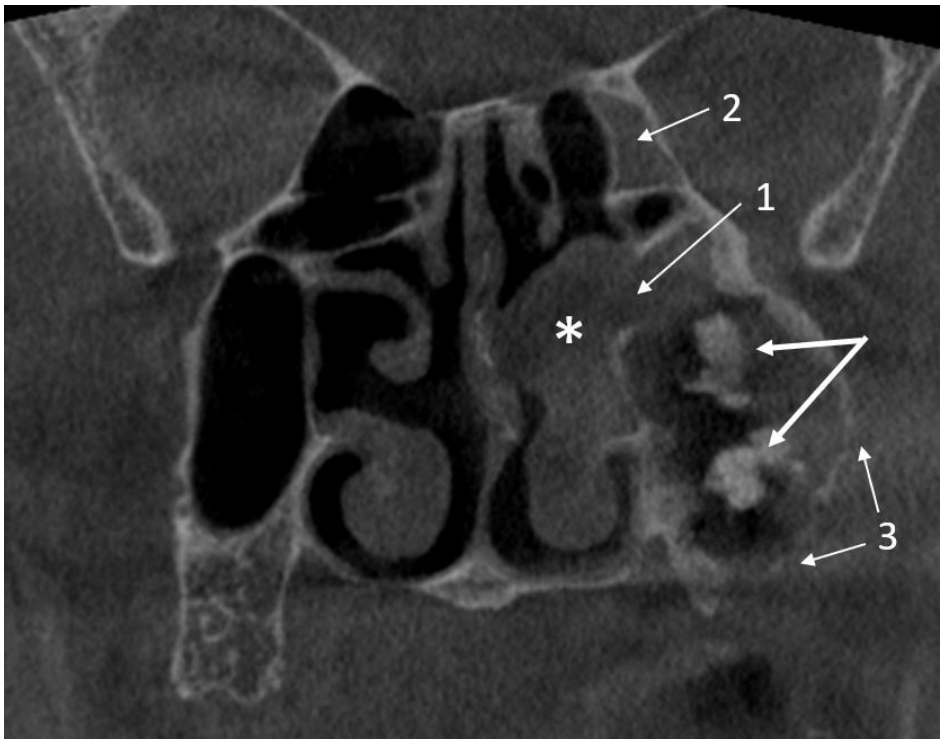

Fig. 41. Patient n°12. (Patient 69 years-old). Planmeca 3D Mid. Coronal view of the posterior area of the posterior complex odontoma. Arrows: amorphous tissue belonging to the posterior complex odontoma. 1. Upper nasal wall missing on the left maxillary sinus. (*) thickening of the mucosa around the left middle turbinate. 2. Thickening of the mucosa in the posterior cells of the left ethmoid sinus. 3. Thinning of the lateral wall of the left maxillary sinus.

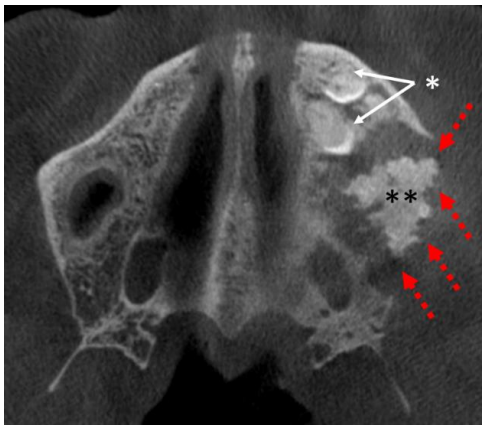

Fig. 42. Patient n°12. (Patient 69 years-old). Planmeca 3D Mid. Axial view of complex odontoma at the level of the floor of the left maxillary sinus. (*) Denticules component of the anterior complex odontoma. (**) Amorphous component of the posterior complex odontoma. Red discontinuous arrows: absence of left lateral wall of the left maxillary sinus with the complex odontoma in eruptive state.

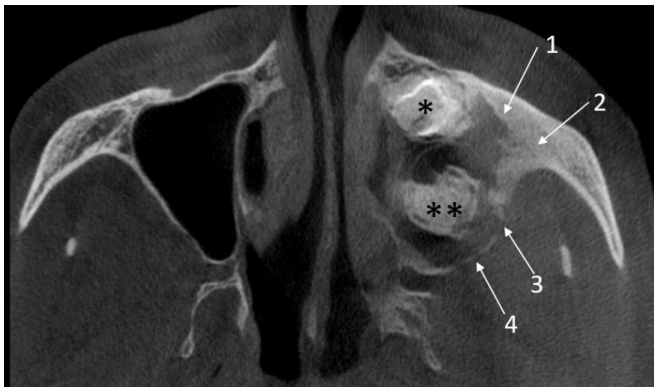

Fig. 43. Patient n°12. (Patient 69 years-old). Planmeca 3D Mid. Axial view at the midsection of the anterior (*) and posterior (**) complex odontoma. Amorphous and denticule content of the anterior complex odontoma (*). Amorphous only content of the posterior complex odontoma (**). 1. Erosion of the left zygomaticomaxillary process. 2. Hyperostosis of the left zygomaticomaxillary process.

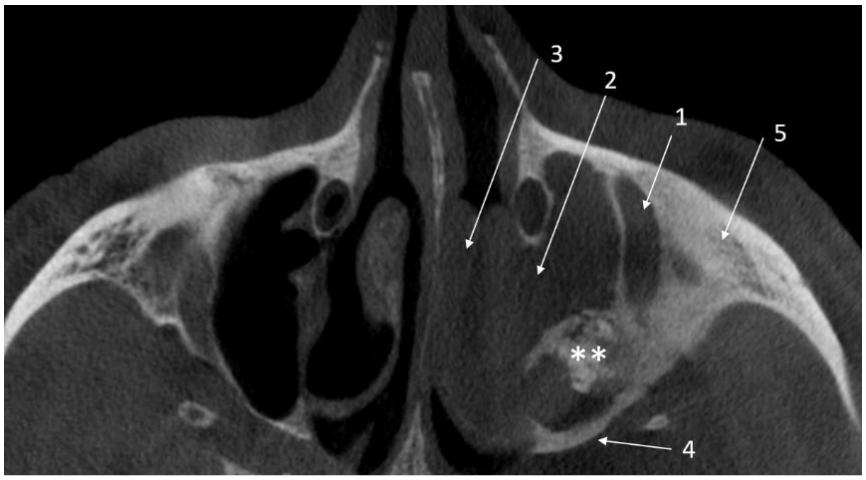

Fig. 44. Patient n°12. (Patient 69 years-old). Planmeca 3D Mid. Axial view at the upper level of the complex odontoma. (**) Posterior complex odontoma. 1. Left suborbital nerve canal with posterior contact with the posterior complex odontoma (**). 2. Absence of the nasal wall of the left maxillary sinus. 3.Thinckening of the mucosa of the left middle turbinate, and obstruction of the left nasal fossa. 4. Hyperostosis of the left lateral wall of the left maxillary sinus. 5. Hyperostosis of the left zygomaticomaxillary process.

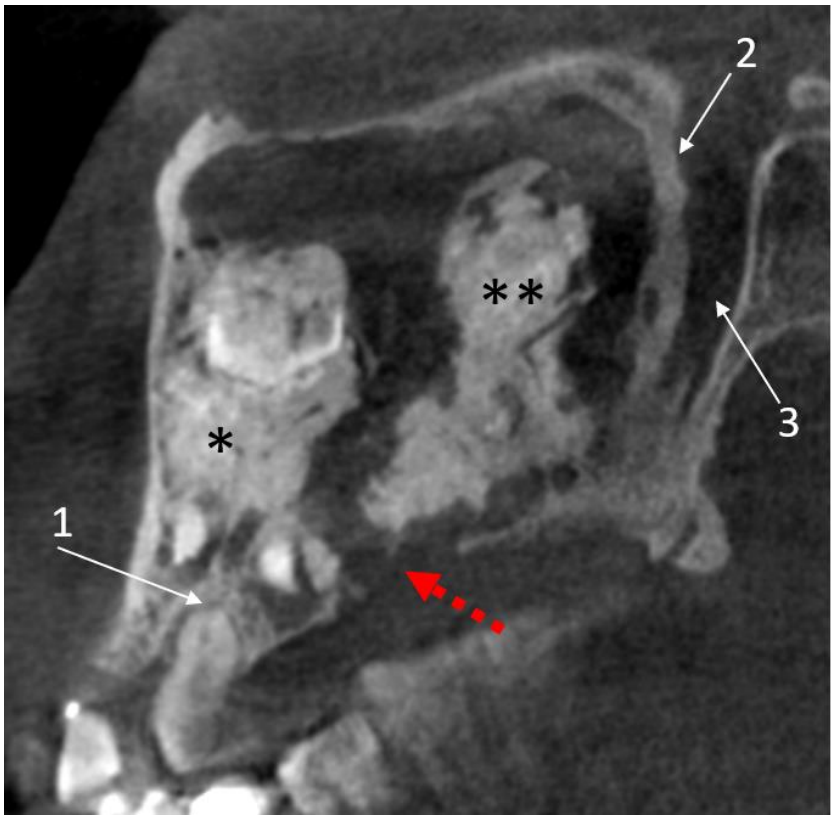

Fig. 45. Patient n°12. (Patient 69 years-old). Planmeca 3D Mid. Sagittal view close to the nasal wall of the left maxillary sinus. Anterior (*) and posterior (**) complex odontoma. Red discontinuous arrow: perforation of the palatine bone and oro-antral communication. 1. External resorption of the tooth n° 15 by the anterior complex odontoma. 2. Hyperostosis of the posterior wall of the left maxillary sinus. 3. Left great palatine canal.

Fig. 46. Patient n°12. (Patient 69 years-old). Planmeca 3D Mid. Sagittal view through the midline of both odontoma. (*) Anterior complex odontoma. (**) Posterior complex odontoma. Red discontinuous arrows: perforation of the alveolar bone of the left maxilla, and posterior complex odontoma in eruptive state. 1. Left suborbital nerve foramen and canal surrounded by the anterior complex odontoma. 2. Hyperostosis of the floor of the left orbit. 3. P-Left pterygopalatine fossa.

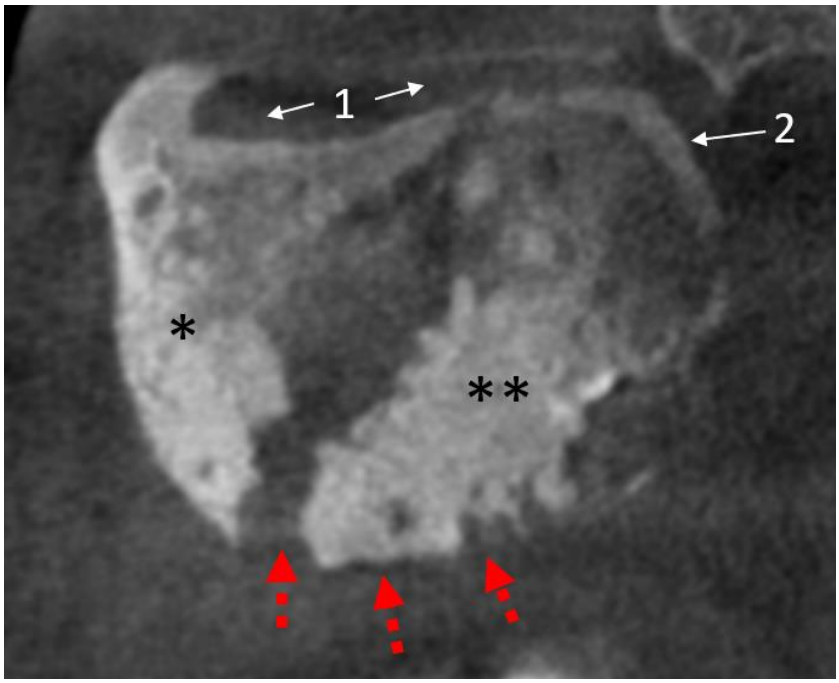

Fig. 47. Patient n°12. (Patient 69 years-old). Planmeca 3D Mid. Sagittal view through the lateral wall of the left maxillary sinus. (*) Anterior complex odontoma. (**) Posterior complex odontoma. Red discontinuous arrows: perforation of the lateral wall of the left maxillary sinus, and posterior complex odontoma in eruptive state. 1. Left suborbital nerve canal surrounded by hyperostotic bone. 2. Hyperostosis of the posterior wall of the left maxillary sinus.

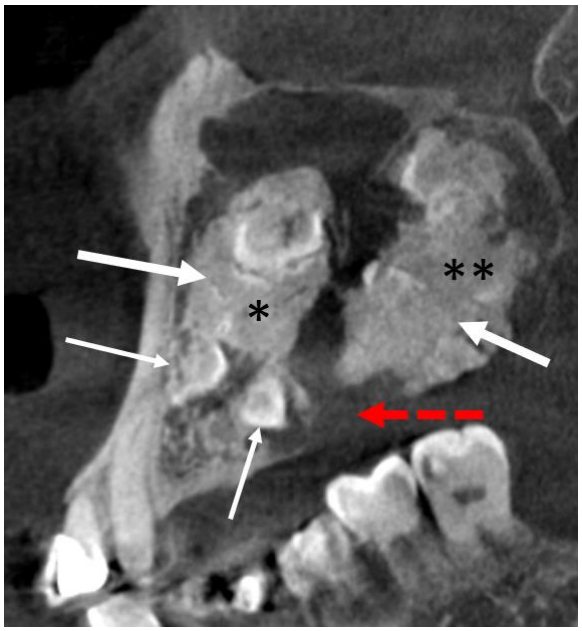

Fig. 48. Patient n°12. (Patient 69 years-old). Planmeca 3D Mid. Multi-reformatted sagittal view through both the anterior and posterior complex odontoma. Anterior complex odontoma (*) and posterior complex odontoma (*). Red discontinuous arrow: perforation of the alveolar bone of the left maxilla, and left oro-antral communication. Thick arrows: amorphous content of the complex odontoma. Thin arrows: denticule content of the complex odontoma.

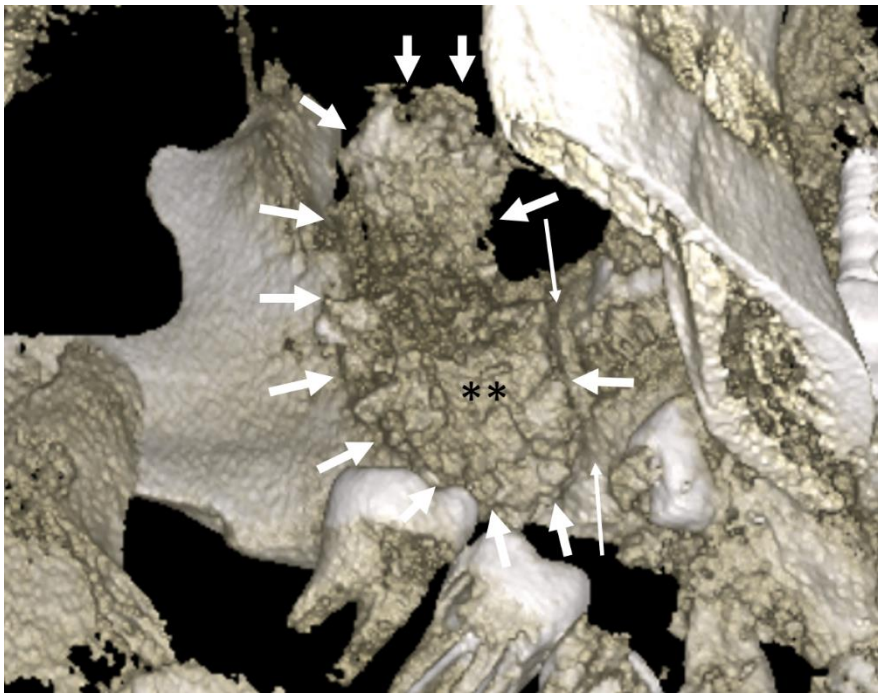

Fig. 49. Patient n°12. (Patient 69 years-old). Planmeca 3D Mid. 3D reconstruction of the posterior complex odontoma (**) with its limits underlined with thick arrows. Thin arrows: border between both odontomas.

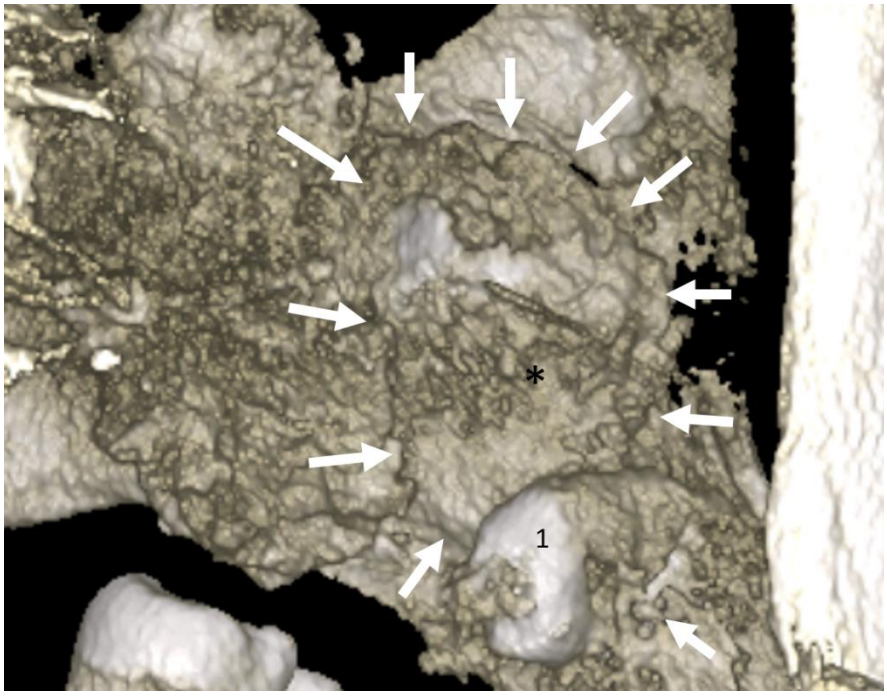

Fig. 50. Patient n°12. (Patient 69 years-old). Planmeca 3D Mid. 3D reconstruction of the anterior complex odontoma (*) with its limits underlined with thick arrows. 1. Denticule component of the complex odontoma.

Discussion

Odontomas are the most common benign odontogenic tumours with a histologically high degree of differentiation and an excellent biological behaviour. They may occur in two forms: a complex odontoma or a compound odontoma [24]. A complex odontoma looks like an irregular and disorganized mass of tooth tissue and occurs mainly in the premolar-molar region of the upper and lower jaw. On the other hand, a compound odontoma is a conglomerate of numerous small fragments. Many of these fragments are real miniature teeth in which a crown and a root, covered by enamel and cementum, can be clearly distinguished. The number of these tooth-like configurations can vary from a few individuals to several hundred [25]. In this discussion, the radiological features of odontomas will firstly be discussed, followed by the difficulties of diagnosis and why a CBCT classification matrix is of great value. Lastly, the role of CBCT in treatment and treatment planning will be discussed.

Radiologic features

Radiologically, this odontogenic tumour is initially lucent, but with time, it develops small calcifications, which eventually coalesce to form a radio-dense lesion with a lucent rim [26]. Compound odontomas usually contain a radio-opaque mass with irregular margins and tooth-like structure. Compound odontomas present radio-lucid peripheral borders, whereas complex odontomas exhibit unique radio-opacity, sometimes surrounded by a thin radiolucent area [1, 25, 27]. According to the degree of odontoma calcification, three stages of development can be identified: 1) radio-lucid stage lacking calcification of dental tissues, 2) stage with partial calcifications, and 3) radio-opaque stage surrounded by a radio-lucid halo [25, 28]. Orthopantomogram, periapical, and occlusal radiographs are conventional dental radiography techniques which are commonly used for diagnostic purpose. But, CBCT provides several advantages regarding diagnostic and treatment planning because it provides a three-dimensional image of the structural relationships. Images in three planes of sections (axial, sagittal, coronal) make evaluation of anatomical structures more accurate, and 3D reconstruction can play a critical role in diagnosis and surgical panning [1, 2]. Moreover, it provides the determination of the tumour size, density, presence of root resorption, cortical bone expansion, and perforation, in addition to the relationship with adjacent anatomic structures such as the inferior alveolar nerve and adjacent teeth [29]. Both the extent of the lesion and its effects on adjacent structures are better delineated with CBCT. Additionally, the presence of calcifications and cortical perforation are more visible on CBCT versus a panoramic image [2].

Diagnosis

Problems concerning the diagnosis are related to the site (multiple or unique), size and location of the odontoma. The location can be intraosseous, extraosseous (partially or completely) and rarely in soft tissues. [1, 2, 10-12, 15-22] Furthermore, extension of the lesion can be bony expansion, thinning or perforation of the cortical bone. These extensions are better visible on CBCT [4, 6, 30]. Lastly, the relationship between the odontoma and adjacent teeth and adjacent structures are of importance for the diagnosis [2, 30]. Since CBCT offers a precise position and accurate diagnosis of complex and compound odontomas this research constructed a classification matrix for complex and compound odontomas [1, 4, 6].

Classification matrix

This open classification matrix for compound and complex odontomas on Table 1 contains 102 boxes. The descriptions for our classification matrix were composed of: 1) Giant odontoma; 2) Quantity; 3) Location within the arch; 4) Location in relation with adjacent teeth; 5) Maxilla location; 6) Mandible location; 7) Type; and 8) Complications. According to our clinical findings (Figures 20, 33, 34, 36) we added two new sub-classifications for "location within in arch": Pre-erupted state

(perforation of alveolar bone on the dental arch), and partially extragnathic position of odontoma. The "location in relation with adjacent definitive teeth" was also added, based on the same scheme as the location in relation with adjacent deciduous teeth from Teruhisa et al. [23]. Furthermore, we added 7 new subclassifications for description of the position of the odontoma in relation with the definitive tooth. We added mandible and maxilla location separated into anterior, premolar, and molar area that were not present in previous classifications. We added the denticulo-amorphous type according to our clinical findings (Figures 15, 18, 22-25, 42, 43, 45-48, 50). Finally, we added 12 new sub-classifications on complications related to odontomas.

The content of the presented matrix is based on descriptions of odontomas in open-access literature, from authors' interpretation of figures and illustrations in the open-access selected articles and from own presented cases. The 36 boxes were already illustrated by 23 figures available in open-access literature in Pubmed [7, 10-22]. This article freely provided 50 figures. The open access figures from literature and from this research illustrated 23 boxes. With this pictorial review, this research was able to illustrate itself 30 boxes. In the future, other authors could complete 30 empty boxes, add more types in the same classification or add new (sub)classifications below or inside the existing ones presented in this research. Analogically, new research could be published in open-access.

Therefore, this pictorial review was able to freely provide the readership with a more complete description of complex odontomas, compound odontomas, multiple compound odontomas and double extragnathic complex odontomas on CBCT data in comparison to earlier published studies.

Treatment and treatment planning

After surgical removal of odontoma, there is no tendency of recurrence. Nevertheless, it is advisable to always have the surgical specimen examined anatomically because of the rare possibility of an odonto-ameloblastoma. This rare lesion combines the characteristics of an odontoma with those of an ameloblastoma. Treatment is identical to that of an ameloblastoma. According to WHO (2017), odonto-ameloblastoma no longer forms a separate entity but is included in ameloblastoma.

When odontomas extend beyond the alveolar process into the fascial planes, nasal fossae, paranasal sinuses, and orbits, a CBCT can more precisely demonstrate the extent and boundaries of the lesions. For example, a compound odontoma can cause a slight bone expansion that is noticeably different from the more significant bone expansion caused by complex odontoma [31]. Moreover, CBCT imaging allows a 3D visualization that, besides showing the association between lesions, also demonstrates the margins of the connected lesions and their internal architecture, and provides a precise follow-up after surgical removal [2, 32]. A prompt follow-up is essential for evaluation of further development of the permanent dentition at the removal location [2]. Additionally, CBCT imaging provides a detailed assessment of

675 odontomas and impacted teeth regarding position, distance to associated teeth and
676 adjacent cortex, and occurrence of root resorption. Moreover, in patients with
677 skeletal malocclusion caused by odontoma, the prioritization of treatment is of great
678 importance. If surgical removal of odontoma is postponed, the probability of
679 adjacent teeth impaction, and therefore malocclusion, increases. Also, it can
680 compromise facial growth and cause facial asymmetry [33, 34]. Therefore, early
681 diagnosis regarding impacted tooth is necessary in order to treat the impacted tooth
682 with for example an orthodontic appliance [35].
683
684 ## Conclusion
685
686 In conclusion, CBCT offers precise position and accurate diagnosis of complex
687 and compound odontomas, while providing important information on treatment
688 management and follow-up that isn't apparent on 2D imaging. Therefore, this
689 review presents a CBCT classification matrix for odontomas describing 1) Giant
690 odontoma; 2) Quantity; 3) Location within the arch; 4) Location in relation with
691 adjacent teeth; 5) Maxilla location; 6) Mandible location; 7) Type; 8) Complications.
692 Consequently, this pictorial review can freely provide the readers a classification
693 matrix with a more complete description of complex and compound odontomas
694 using CBCT data published in earlier studies together with our own clinical cases.
695
696

- **Acknowledgements**: none
- **Funding sources statement**: the study does not receive any funding.
- **Competing interests**: Prof R. Olszewski is Editor-in-Chief of NEMESIS. The other authors declare no conflicts of interest.
- **Ethical approval**: we obtained the approval from our University and Hospital Ethical Committee for this study (B403/2019/03DEC/542)
- **Informed consent**: Patients n°4, 7, 11, 12 were exempted from the informed consent according to the ethical committee approval. There was no need for the informed consent for patients n°1-3, 5, 6, 8-10 as all the images were anonymized and no private data were provided allowing the patient's identification.

Authors contribution:

Author	Contributor role
Dubron Kathia	Conceptualization, Investigation, Methodology, Data curation, Validation, Writing original draft preparation, Writing review and editing
Gurniak Anna	Data curation, Validation, Writing review and editing
Gurniak Eliza	Data curation, Validation, Writing review and editing
Politis Constantinus	Validation, Writing review and editing
Olszewski Raphael	Conceptualization, Investigation, Methodology, Data curation, Resources, Validation, Writing original draft preparation, Supervision, Writing review and editing

References

1. Millan JPD, Gutinik, BC, Lima LLM. de Teles AKG, Martins TA, Tempest LM. Odontomas and imaging diagnosis: the concise systematic review. MedNEXT J Med Health Sci 2021;2. https://doi.org/10.54448/mdnt21504.

2. Iatrou I, Vardas E, Theologie-Lygidakis N,Minas Leventis M. A retrospective analysis of the characteristics, treatment and follow-up of 26 odontomas in Greek children. J Oral Sci 2010;52:439-447. https://doi.org/10.2334/josnusd.52.439.

3. De Vos W, Casselman J, Swennen GR, Cone-beam computerized tomography (CBCT) imaging of the oral and maxillofacial region: a systematic review of the literature. Int J Oral Maxillofac Surg 2009;38:609-625. https://doi.org/10.1016/j.ijom.2009.02.028.

4. Satish V, Prabhadevi MC, Sharma R. Odontome: A brief overview. Int J Clin Pediatr Dent 2011;4:177-185. https://doi.org/10.5005/jp-journals-10005-1106.

5. Wright JM, Soluk Tekkesin M. Odontogenic tumors: where are we in 2017? J Istanb Univ Fac Dent 2017;51:S10-S30. https://doi.org/10.17096/jiufd.52886.

6. Pacifici A, Carbone D, Marini R, Pacifici L. Surgical management of compound odontoma associated with unerupted tooth. Case Rep Dent 2015;2015:902618. https://doiorg/10.1155/2015/902618.

7. Amado Cuesta S, Gargallo Albiol J, Berini Aytés L, Gay Escoda C. Review of 61 cases of odontoma. Presentation of an erupted complex odontoma. Med Oral 2003;8:366-373.

8. Kara, M.I, Ay S, Aktan AM, Sener I, Bereket C, Ezirganli S, Demirkol M. Analysis of different type of transmigrant mandibular teeth. Med Oral Patol Oral Cir Bucal2011;16:e335-e340. https://doi.org/10.4317/medoral.16.e335.

9. Mortazavi H, Baharvand M, Rahmani S, Jafari S, Parvaei P. Radiolucent rim as a possible diagnostic aid for differentiating jaw lesions. Imaging Sci Dent 2015;45:253-261. https://doi.org/10.5624/isd.2015.45.4.253.

10. Augusto-Neto RT, Marinheiro BH, Silveira HA, Polanco XBJ, León JE, Trivellato AE, Sverzut CE. Complex odontoma restricting mouth opening: an unusual clinical presentation and surgical management. Int J Health Sci (Qassim) 2021;15:60-63.

11. Santos LA, Lopes LJ, Roque-Torres GD, Oliveira VF, Freitas DQ. Complex odontoma: A case report with micro-computed tomography findings. Case Rep Dent 2016;2016:3584751. https://doi.org/10.1155/2016/3584751.

12. Miura K, Miyashin M, Kanao T, Oishi A. Eruption disturbance caused by an odontoma that was partially attached to the crown of the adjacent maxillary first molar, and step lesion excavation for the tooth preservation: A case report. Clin Case Rep 2019;7:2462-2465. https://doi.org/10.1002/ccr3.2523.

13. Ćabov T, Fuchs PN, Zulijani A, Ćabov Ercegović L, Marelić S. Odontomas: pediatric case report and review of the litterature. Acta Clin Croat 2021;60:146-152. https://doi.org/10.20471/acc.2021.60.01.22.

14. Bagewadi SB, Kukreja R, Suma GN, Yadav B, Sharma H. Unusually large erupted complex odontoma: A rare case report. Imaging Sci Dent 2015;45:49-54. https://doi.org/10.5624/isd.2015.45.1.49.

15. Flores Orozco EI, Abu Hasna A, Teotonio de Santos Junior M, Flores Orozco EI, Falchete Do Prado R, Rocha Campos G, Carneiro Valera M. Case report: Inter-disciplinary management of a complex odontoma with a periapical involvement of superior anterior teeth. F1000Res. 2019;8:1531. https://doi.org/10.12688/f1000research.20337.1

16. Kannan KS, Prabhakar R, Saravanan R, Karthikeyan, Rajvikram. Composite compound odontoma-a case report. J Clin Diagn Res 2013;7:2406-2407. https://doi.org/10.7860/JCDR/2013/7432.3540.

17. Poli PP, Creminelli L, Grecchi E, Pieriboni S, Menozzi G, Maiorana C. Anxiolysis in the surgical management of a compound odontoma in a pediatric patient. Case Rep Den. 2019;2019:1385150. htpps://doi.org/10.1155/2019/1385150.

18. Oda M, Nishida I, Habu M, Takahashi O, Tsurushima H, Otani T, Yoshiga D, Saeki K, Tanaka T, Wakasugi-Sato N, Matsumoto-Takeda S, Nagasaki Y, Miyamoto I, Kito S, Sasaguri M, Morimoto Y. Overview of radiological studies on visualization of gubernaculum tracts of permanent teeth. J Clin Med 2021;10:3051. https://doi.org/10.3390/jcm10143051.

19. Borghesi A, Tonni I, Pezzotti S, Maroldi R. Peripheral osteoma, compound odontoma, focal cemento-osseous dysplasia, and cemento-ossifying fibroma in the same hemimandible: CBCT findings of an unusual case. Radiol Case Rep 2017;12:756-759. https://doi.org/10.1016/j.radcr.2017.08.011.

20. Hashim HA, Al-Qahtani AA, Taha SM, Tharupeedikayil S, Ahmed MF.

Management of complete impacted maxillary second deciduous molar with the aid of cone-beam computed tomography: Case report and a review of the literature. J Orthod Sci 2013;2:130-135. https://doi.org/10.4103/2278-0203.123201.

21. Janarthanan K, Thangavelu A, Adalarasan S, Selvakumar R, Murugan R, Reddy SV. Impacted upper lateral incisor in a 16-year-old female-"Compound Odontome" the culprit-A case report. J Pharm Bioallied Sci. 2019;11:S488-S490. https://doi.org/10.4103/JPBS.JPBS_3_19.

22. Jung YH, Kim JY, Cho BH. The effects of impacted premaxillary supernumerary teeth on permanent incisors. Imaging Sci Dent 2016;46:251-258. https://doi.org/10.5624/isd.2016.46.4.251.

23. Teruhisa U, Murakami J, Hisatomi M, Yanagi Y, Asaumi J. A case of unerupted lower primary second molar associated with compound odontoma. Open Dent J 2009;3:173-176. https://doi.org/10.2174/1874210600903010173.

24. Tsiklakis K, Spyropoulos ND. [Radiographic study of odontomas]. Odontostomatol Proodos 1990;44:117-123.

25. ThistleBarba L, Muela Campos D, Nevárez Rascón MN, Ríos Barrera VA, Nevárez Rascón A. Descriptive aspects of odontoma: literature review. Revista Odontológica Mexicana 2016;20:e265-e269. https://doi.org/10.1016/j.rodmex.2016.11.018

26. Gervasoni C, Tronchet A, Spotti S, Valsecchi S, Palazzolo V, Riccio S, Aiuto AD, Azzi L, Di Francesco A. Odontomas: review of the literature and case reports. J Biol Regul Homeost Agents 2017;31:119-125.

27. Soluk Tekkesin M, Pehlivan S, Olgac V, Aksakalli N, Alatli C. Clinical and histopathological investigation of odontomas: review of the literature and presentation of 160 cases. J Oral Maxillofac Surg 2012;70:1358-1361. https://doi.org/10.1016/j.joms.2011.05.024

28. Hisatomi M, Asaumi JI, Konouchi H, Honda Y, Wakasa T, Kishi K. A case of complex odontoma associated with an impacted lower deciduous second molar and analysis of the 107 odontomas. Oral Dis 2002;8:100-105. https://doi.org/10.1034/j.1601-0825.2002.1c778.x

29. Dhont K, Bernaerts A, Vanhoenacker Ch, Vanhoenacker FM, De Foer B. Imaging anatomy of the jaw and dentition with cone beam computed tomography. Semin Musculoskelet Radiol 2020;24:488-498. https://doi.org/10.1055/s-0040-1701494.

30. Indermun S, Shaik S, Opperman J. A bunch of grapes with a bag of marbles: The concurrence of the botryoid odontogenic cyst with a compound odontoma. Oral Surgery 2021;14:349-357. https://doi.org/10.1111/ors.12581.

31. Sikes Jr JW, Ghali GE, Troulis MJ. Expansile intraosseous lesion of the maxilla. J Oral Maxillofac Surg 2000;58:1395-1400. https://doi.org/10.1053/joms.2000.18274.

32. Marques YM, Botelho TD, Xavier FC, Rangel AL, Rege IC, Mantesso A. Importance of cone beam computed tomography for diagnosis of calcifying cystic odontogenic tumour associated to odontoma. Report of a case. Med Oral Patol Oral Cir Bucal 2010;15:e490-493. https://doi.org/10.4317/medoral.15.e490.

33. Kadlub N, Kreindel T, Mbou VB, Amélie Coudert A, Edward Ansari E, Descroix V, Ruhin-Poncet B, Coulomb L'hermine A, Berdal A, Vazquez MP, Ducou Lepointe H, Picard A. Specificity of paediatric jawbone lesions: tumours and pseudotumours. J Craniomaxillofac Surg 2014;42:125-131. https://doi.org/ 10.1016/j.jcms.2013.03.007.

34. Pithon MM. Nonsurgical treatment of severe Class II malocclusion with anterior open bite using mini-implants and maxillary lateral incisor and mandibular first molar extractions. Am J Orthod Dentofacial Orthop 2017;151:964-977. https://doi.org/ 10.1016/j.ajodo.2016.04.035.

35. Cozza P, Gatto R, Marino A, Mucedero M. Case report: two nasal floor compound odontomas associated with impacted maxillary incisor. Eur J Paediatr Dent 2003;4:99-102.